Denitrification rates by free and encapsulated microorganisms under different environmental pressures

A thesis submitted in partial fulfilment of the requirements for the Degree of Master of Engineering

in the University of Canterbury

by

Zhe (Turin) Li

Department of Civil and Natural Resource Engineering

College of Engineering

University of Canterbury, New Zealand

2020

Acknowledgment

First and foremost, I would like to express my sincere gratitude to my research supervisors Dr Ricardo Bello Mendoza and Dr David Wareham, Department of Civil and Natural Resources Engineering (CNRE), University of Canterbury, New Zealand, for offering me the opportunity of doing this research and their priceless intellectual guidance in my experimental and writing work. You have shown me, with your vision, sincerity and motivation, what a good scientist should be. It was a great privilege to work and study under your guidance.

I am grateful to those who also helped and guided me during my research, especially to the technical advisors in the environmental laboratory: Mr. Peter McGuigan, Mr. Manjula Premaratne and Dr Aude Thierry. As you were always willing and able to help me solve any problem that occurred during my lab work, I could go smoothly through all my experiments.

Please allow me to give special appreciation to Dr Simone Larcher and Dr Mark Milke for offering me casual job opportunities so I could be relieved from the financial burden as an international student.

I would like to take this opportunity to thank my UC friends for their support, including Afrooz Bayat, Ethar Al-Essa, Forrest Bilek, Fabio Silveira, Farideh Jamalibehnam, Rohit Gokhale, Abhirup Basu Roy Chowdhary, Lei Zhang, Rondo Law, Elizabeth North, Janguk Aidan Lee, Jongwoo Kim, Thomas Wallace and Yanina Ferligoj. I had a great time with you all and those moments will always be precious in my heart.

Last but not least, I thank my mother and other family members for their encouragement throughout my research.

Zhe Li

Abstract

Nitrate is a water pollutant of concern and its concentration in New Zealand's water bodies has shown an increasing trend during the past three decades due in part to its insufficient removal from wastewater before discharge. Nitrate is commonly removed from wastewater by biological means, in a process known as denitrification. Many environmental factors, such as pH and toxic substances, can affect the biological denitrification process. Cell-encapsulation technology has been claimed to provide protection to microorganisms under hash environmental conditions. However, there is still a need for investigating nitrate removal using encapsulated cells under suboptimal pH conditions and in the presence of potentially toxic organic and inorganic substances. Therefore, the aim of this research was to examine denitrification rates by free suspended cells and cells encapsulated in alginate under different pH levels and different concentrations of nZVI and clopyralid.

The research took place in four phases: Phase I (Preliminary tests), Phase II (Batch tests under different pH conditions), Phase III (Batch tests under different nZVI concentrations), and Phase IV (Batch tests under different clopyralid concentrations). The aim of Phase I was to stablish and operate an anoxic sequencing batch reactor (SBR) as a sludge (i.e. denitrifying biomass) generator for smaller batch tests. However, the SBR failed to attain adequate anoxic, denitrifying conditions as assessed from oxidation-reduction potential (ORP) values in the SBR being regularly around -300 mV and observed spikes of nitrate-nitrogen at the beginning of denitrification tests. Therefore, a decision was made to collect sludge from a nutrient removal WWTP which had a reasonable biomass-specific denitrification rate of 0.114 mg N/(g VSS·min) and to use this sludge as inoculum in subsequent batch tests (Phases II, III, and IV).

In Phase II, the denitrification rate of freely suspended cells was observed to be negatively affected by too low (5.0) or too high (9.3) pH values. In both cases, the biomass specific denitrification rate was similar and around 0.058 ± 0.005 mg N/(g VSS·min). Contrary to the expectation, the denitrification activity of the encapsulated cells appeared to be even more affected than the free cells under all pH conditions.

In Phase III, the biomass-specific denitrification rate of the freely suspended cells was found to be severely affected by the addition of nZVI nanoparticles at concentrations of 0.5 and 3 mg/L. A similar denitrification rate of about 0.023 mg N/(g VSS·min) was observed in both cases. However, the denitrification rate (0.007 mg N/(g VSS·min)) of the encapsulated cells exposed to 0.5 g/L of nZVI was the lowest.

In Phase IV, the denitrification rates were 0.027 and 0.010 mg N/(g VSS·min) for biomass exposed to 50 and 300 mg/L of the herbicide clopyralid. The denitrification rate was more severely impacted by a high clopyralid concentration as compared to a low concentration. The denitrification rate by the encapsulated cells was also affected by the exposure to 50 mg/L of clopyralid. However, in this case, the denitrification rate was twice the rate observed with the free-cells.

Overall, this study confirms the negative effect on the biological denitrification process by suboptimal environmental conditions (i.e. high and low pH, nZVI and clopyralid). However, the expected enhancement caused by cell encapsulation was only observed in the 50 mg/L clopyralid case. In all other cases, cell encapsulation further affected the biological denitrification rates.

Table of contents

List of Figures

List of Tables

1. Introduction

Nitrogen is an important nutrient that plays a key role in agricultural crop production. However, if discharged in large quantities into water bodies it can become a pollutant that cause eutrophication (Lu, Mei Lee, Ming Lu & Chen, 1994). This happens because when nitrogen is introduced into water bodies through point or nonpoint sources, it is taken up by plankton and algae triggering their explosive growth (Parliamentary Commissioner for the Environment, 2013). Nitrogen usually enters the water bodies as nitrate and ammonia (Ministry for Environment, 2007). High levels of total nitrogen can cause algal bloom and red tide phenomena, which can lead to dissolved oxygen depletion (Ministry for Environment, 2007). Enrichment of a water body with nitrogen can finally result in the death of fish and other aquatic organisms. In order to prevent such situations, nitrogen should be removed from wastewaters before being discharged into water bodies.

According to the Australian and New Zealand Guidelines for Fresh and Marine Water Quality (2000), the default trigger value for total nitrogen (TN) for slightly disturbed ecosystems in New Zealand is 295 µg/L. As shown in Fig 1.1, the Ministry for Environment (2007) has reported that the highest and median levels of nitrogen in New Zealand increased slightly over 1985 to 2005 period. Furthermore, nitrogen levels have increased more rapidly in already nutrient-enriched water bodies (Ministry for Environment, 2007).

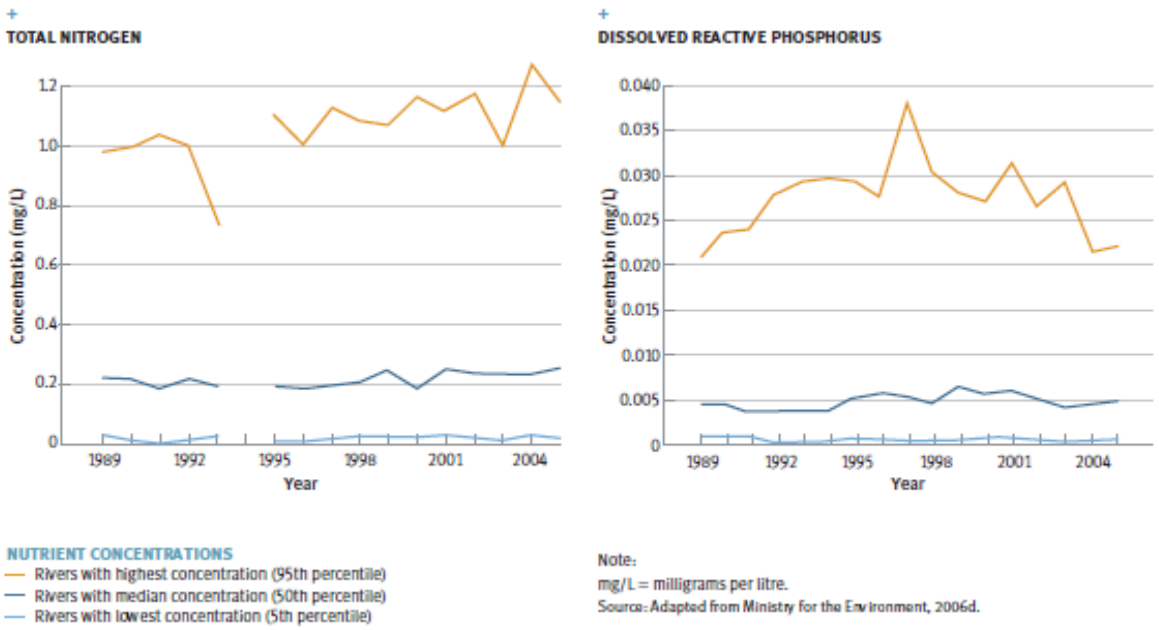

Figure 1.1: Nutrient trends in rivers in the national monitoring network, 1985-2005 (Ministry for Environment, 2007)

According to the 2018 Annual Groundwater Quality Survey conducted by Environment Canterbury (2018), nitrate nitrogen concentration in groundwater vary from 0.05 to 25 mg/L (median value is 3.3 mg/L) which is approximately 16 times as high as the median level from 1985 to 2005. Additionally, Figure 1.2 from this survey suggests that 42 out of 229 wells have an increasing nitrate-concentration trend (Environment Canterbury, 2018). Meanwhile, only 11 wells reported to have decreased nitrate concentrations (Environment Canterbury, 2018).

In order to remove nitrogen from wastewater, many technologies have been researched, developed, and utilised based mainly on the activated sludge process. During the past two decades, most research has investigated this process under different environmental conditions; however, there is still a need for assessing the denitrification performance of immobilised cells, which a popular technology (Mallick, 2002).

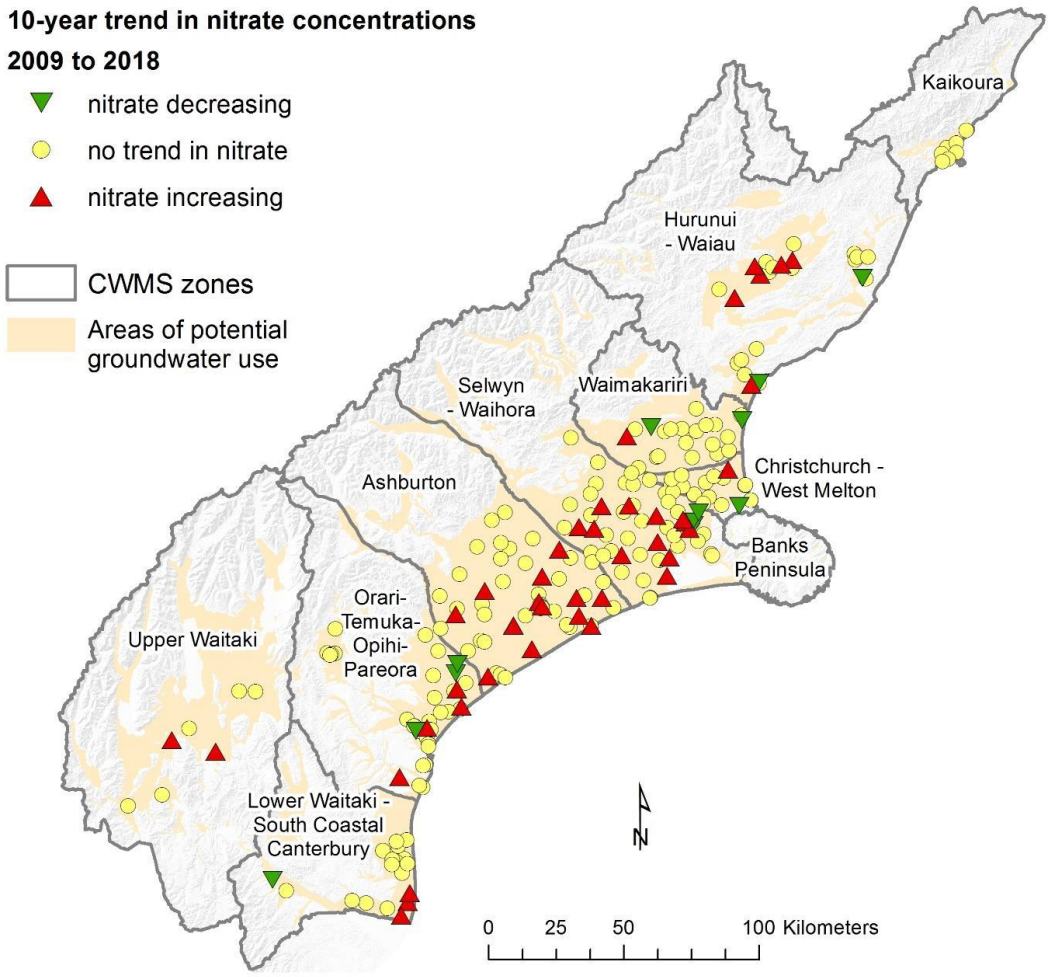

Figure 1.2: Ten-year trends (2009 to 2018) in nitrate concentrations in annual survey wells in Canterbury (Environment Canterbury, 2018)

2. Literature review

2.1. Denitrifying bacteria

Denitrifying bacteria play a key role in removing nitrate-nitrogen from wastewater. The biological denitrification process has been both extensively studied and put into practice, since the original three-stage biological nitrogen removal system was first designed by Edwin Barth in 1969 (Barth, 1972). Molecular oxygen is the most efficient electron acceptor for bacteria to use in the presence of organic electron donors; however, nitrate becomes the terminal electron acceptor in the absence of oxygen (Lee et al., 2000). A simplified anoxic denitrification pathway is as follows: $NO_3^- \rightarrow NO_2^- \rightarrow NO \rightarrow N_2O \rightarrow N_2$ (Lee et al., 2000), with the redox balance of denitrification being: $2NO_3^- + 10e^- + 12H^+ \rightarrow N_2 + 6H_2O$ (Skiba, 2008). Several stoichiometric equations for heterotrophic denitrification with acetic acid are listed in Table 2.1. Accordingly, the optimal COD/N ratio for nitrate removal should be approximately 5:1 (Sobieszuk & Szewczyk, 2006).

Table 2.1: Stoichiometric relationships for heterotrophic denitrification with acetic acid

Stoichiometric Equation	Reference
$0.625CH_3COO^- + 1NO_3^- + 0.375H^+ \rightarrow 1.25HCO_3^- + 0.5N_2 + 0.5H_2O$	Glass & Silverstein (1998)
$5CH_3COOH^- + 8NO_3^- \rightarrow 8HCO_3^- + 2CO_2 + 6H_2O + N_2$	Burghate & Ingole (2014)
$0.819CH_3COOH^- + 1NO_3^- \rightarrow 0.068C_5H_7NO_2 + 1HCO_3^- + 0.301CO_2 + 0.902H_2O + 0.466N_2$	Burghate & Ingole (2014)

2.2. Role of pH in biological denitrification

According to the redox balance of denitrification in Table 2.1, pH can affect the denitrification process with the optimal pH range for biological denitrification reported to be 6.0 - 8.0 (Knowles, 1982; Wang et al., 1995). Previous studies suggest that the inhibition of denitrifying microorganisms under different pH conditions ($6 < pH < 9$) is basically caused by the toxicity of accumulated nitrite and free nitrous acid during denitrification (Chen et al., 1991; Glass et al., 1997). Many studies focused on investigating the effects caused by accumulated nitrite and free nitrous acid on biological denitrification process within the optimal pH range (Pan, Ye, Ni, & Yuan, 2012; Glass & Silverstein, 1998; Cao, Qian & Meng 2012). As reported by Pan et al. (2012), the highest nitrate-removal rate was 45 mg N/(g VSS·hour) at pH 7.0, while the rate dropped by approximately 17 % and 50 % compared to its maximum level at pH 6.5 and pH 9.0, respectively. Additionally, the denitrification process can be significantly inhibited at low pH (2.5 – 6.0) (Napier and Bustamante, 1988; Silverstein et al., 1993; Randall et al., 1992

and Glass et al., 1997). However, only a few studies have been conducted to investigate denitrification rate under a wide range of pH values.

It seems logical therefore to assess the denitrification performance under suboptimal conditions (i.e. pH < 6 and pH > 8) while simultaneously investigates if there any potential approaches that can enhance the biological denitrification rates at these pH levels.

2.3. Effect of toxic organic compounds on biological denitrification

Clopyralid (3,6-dichloro-2-pyridinecarboxylic acid) is an herbicide of the picolinic acid family and is reported to be highly soluble in water (Tu et al., 2001). According to Shchegolkova et al. (2016) and Hura (2019), clopyralid can affect the degradation of some compounds in wastewaters by inhibiting the activity of microorganisms through damaging the structure of the microbial community of an activated sludge. As reported by Hura (2019), in the range from 50 to 225 mg/L, clopyralid does not affect the microbial activity; although the microorganisms were severely inhibited at a clopyralid concentration of 300 mg/L.

There appears to be no research evaluating the potential effects of clopyralid specifically on biological denitrification in wastewater treatment, suggesting it is reasonable to investigate the effects and potential means to protect denitrifying bacteria against such impacts.

2.4. Biological denitrification in the presence of nanoscale zero-valent iron

Over and above pH and clopyralid, nanoscale zero-valent iron (nZVI) has been reported to have effects on the denitrification process since in aqueous systems, zero-valent iron particles (Fe^0) can be oxidized to ferrous ion (Fe^{2+}) by many oxidants (Yang & Lee, 2005). In this process, the oxidation of Fe^0 to Fe^{2+} is the anodic half-reaction suggesting the available electron acceptors (e.g., H^+ and H_2O) in the same system will be involved in the associated cathodic half reaction. Therefore, the potential process of an anaerobic aqueous ZVI system can be described as follows: (1) $\mathrm{Fe^0 + 2H^+ \rightarrow Fe^{2+} + H_2}$; (2) $\mathrm{Fe^0 + 2H_2O \rightarrow Fe^{2+} + H_2 + 2OH^-}$ (Agrawal and Tratnyek, 1996). Under aerobic conditions, dissolved oxygen however would be the preferred electron acceptor in the cathodic half-reaction making the reaction to be: $\mathrm{2Fe^0 + O_2 + 2H_2O \rightarrow 2Fe^{2+} + 4OH^-}$, which yields only OH^- but no H_2 (Huang and Zhang, 2004). Accordingly, ZVI can affect the H^+ concentration in the system, which may further influence the biological denitrification processes. In addition, nitrate nitrogen can also be an electron acceptor, which suggests that theoretically nitrate can react with ZVI and be removed in this way.

The first study investigating the reactions and relevant mechanisms between nitrate and ZVI, was reported in the mid 1960s (Young et al., 1964). However, research into the reduction of nitrate by ZVI did not become popular until the 1990s. Several studies reported the final products of the chemical reduction of nitrate by ZVI as being N_2 or NH_3 depending upon the

experimental conditions (Flis, 1991; Agrawal and Tratnyek, 1996; Siantar et al., 1996; Chew and Zhang, 1998; Huang et al., 1998; Till, 1998; Hu et al., 1999; Choe et al., 2000; Kielemoes et al., 2000; Alowitz and Scherer, 2002; Huang and Zhang, 2002, 2004). The relevant reaction equations are shown in Table 2.2.

Table 2.2: Reaction equations for nitrate reduction by ZVI

Reaction Equation	Reference
$10Fe^0 + 6NO_3^- + 3H_2O \rightarrow 5Fe_2O_3 + 6OH^- + 3N_{2(g)}$	Flis (1991)
$Fe^0 + NO_3^- + 2H^+ \rightarrow Fe^{2+} + H_2O + NO_2^-$	Siantar et al. (1996)
$5Fe^0 + 2NO_3^- + 6H_2O \rightarrow 5Fe^{2+} + 12OH^- + N_{2(g)}$	Chew & Zhang (1998)
$Fe^0 + NO_3^- + 2H_3O^+ \rightarrow Fe^{2+} + 3H_2O + NO_2^-$	Till et al. (1998)
$4Fe^0 + NO_3^- + 10H_3O^+ \rightarrow 4Fe^{2+} + 13H_2O + NH_4^+$	Huang et al. (1998)
$4Fe^0 + NO_3^- + 7H_2O \rightarrow 4Fe^{2+} + 10OH^- + NH_4^+$	Choe et al. (2000)
$4Fe^0 + NO_3^- + 10H^+ \rightarrow 4Fe^{2+} + 3H_2O + NH_4^+$	Alowitz & Scherer (2002)
$2.82Fe^0 + NO_3^- + 0.75Fe^{2+} + 2.25H_2O \rightarrow 1.19Fe_3O_4 + 0.5OH^- + NH_4^+$	Huang & Zhang (2002)
$8Fe^0 + NO_3^- + 10H^+ \rightarrow 8Fe^{3+} + 3H_2O + NH_4^+$	Huang & Zhang (2004)

The studies mentioned above focus on the chemical reduction of nitrate by nanoscale ZVI; however, the purpose of the present study will be to investigate the effect on biological denitrification processes caused by nZVI and its related mechanisms including the kinetics.

2.5. Cell encapsulation technology

The separation of biomass from treated water can be a major limitation for denitrifying wastewater treatment systems (Mallick, 2002). Immobilization techniques for bacterial cells have been utilised to facilitate the separation of the sludge from treated water for further

processing (de la Noue & de Pauw, 1988). There are six immobilization methods; namely, covalent coupling, affinity immobilization, adsorption, confinement in liquid-liquid emulsion, capture behind semipermeable membrane and entrapment (Mallick, 2002). Among these methods, entrapment (the encapsulation of cells in gel lattices by using synthetic or natural polymers) is the most popular, with the most frequently used gel materials being alginate, polyvinyl alcohol and carrageenan (Mallick, 2002). Although the cells are entrapped, substrates and products can still be taken in and released through the pores of the beads. To form the beads with encapsulated cells, a solution is first prepared by mixing aqueous gel material with cells (Mallick, 2002). Afterwards, in general, the solution is forced through a nozzle and drip fed into a salt solution a droplet at a time (Mallick, 2002). The droplets are stabilised in the salt solution to form beads with encapsulated cells through crosslinking with the metal ions in the salt solution (Mallick, 2002). For example, alginate droplets can be stabilised with Ca^{2+} (Mallick, 2002).

Since the first report on immobilisation of microorganisms was published in 1966 (Park et al., 1966), many studies have been conducted to determine the advantages and disadvantages of entrapment technology. For example, since the microorganisms are separated from the wastewater, immobilisation technology should provide more flexibility in the reactor's design (Pramanik, McEvoy, Siripattanakul & Khan, 2011). Cell immobilisation has several other advantages, including increased cell density, increased cell wall permeability, no washout of cells and better operational stability (Chen, Kao, Chen, Chien & Lin, 2007; Pramanik, S., McEvoy, Siripattanakul & Khan, 2011). These advantages may lead to an acceleration of reaction rates. In terms of growth rate, entrapment may lead to the lag phase being longer than that of free cells (Lau, Tam & Wong, 1997). However, the maximum growth rates of immobilised and free cells have been observed to be similar during the exponential growth phase (Lau et al., 1998; Pramanik & Khan, 2008).

Research has also been conducted to deploy entrapped cells for removal of contaminants such as ammonia and nitrate. As reported by Chevalier & de la Noue (1985), the uptake rate of NH_4^+ is the same for entrapped and free cells. However, in some other cases, the removal rate of nitrogen is reported to be significantly enhanced by the entrapment (Liu, Li, Qiao, Lin & Wang, 2012; Megharaj et al., 1992; Thakur & Kumar, 1999; Tam & Wong, 2000). However, only a few studies have been conducted to investigate the removal of nitrogen by entrapped cells under conditions outside the optimal range of pH and/or in the presence of toxics (Sergio, Covarrubias, Manuel Moreno & Yoav Bashan, 2012; Zhao, Yang, Li, Wang, An, Xie, Xu, Deng & Zeng, 2015). Moreover, most studies onnitrogen removal by entrapped cells investigated nitrification.

2.6. Sequencing batch reactor

All the systems used in the above research are conventional continuous flow activated sludge systems, which suggests that they have similar limitations caused by the variations in the volumetric flow and mass loading (Wilderer, Irvine & Goronszy, 2001). Therefore, the idea of

developing a new technology based on batch-fed system was raised in the 1960s (Artan & Orhon, 2005). This technology, known as the sequencing batch reactor (SBR) process, usually consists of a series of periodic process phases, namely fill, react, settle, decant and idle (Artan & Orhon, 2005). In some cases, the idle phase can be eliminated if there is excess inflow available (Wilderer, Irvine & Goronszy, 2001). According to the energy input to the system, several sub-phases can be added to the fill and react phases (Wilderer, Irvine & Goronszy, 2001). The SBR is basically a single tank that serves both as a biological reactor and settler in a temporal sequence. Due to the simple physical structure, the most striking feature of the SBR process is the system flexibility. Therefore, the SBR is considered to be a perfect experimental vehicle for the investigation of the intricacy of microbial mechanisms associated with different biological wastewater treatment processes (Artan & Orhon, 2005). Normally, the SBR is set up and operated under oxic conditions. However, in some studies, an SBR can be employed to study the nutrient removal performance under anoxic and anaerobic conditions (Vackova, Stloukal & Wanner, 2012).

2.7. Objectives

The aim of this research was to assess the feasibility of using cell encapsulation as a technique to enhance the denitrification process under suboptimal environmental conditions. This included conditions of a high and low pH. Another aim was to evaluate if nanoparticles would improve the denitrification process when the cells were encapsulated. In addition, it was sought to assess whether cell encapsulation would protect denitrifying activity against the toxic effect of the herbicide clopyralid. Correspondingly, this research consisted of 4 major phases with the specific objectives for each phase as follows:

Phase I (Preliminary tests): Establishment of pseudo-steady-state conditions in an anoxic sequencing batch reactor (SBR). The objective of the SBR is to be a sludge generator, providing biomass that exhibits a healthy denitrification rate.

Phase II (Batch tests under different pH conditions) has 3 stages with the corresponding objectives as follows: (1) Stage II-1 (using freely suspended cells): to assess the denitrification rates of freely suspended cells under different pH conditions; (2) Stage II-2 (using abiotic sodium-alginate beads): to investigate if there is potential adsorption and chemical reactions between the nitrate and the sodium-alginate beads under different pH conditions; (3) Stage II-3 (using encapsulated cells): to evaluate the denitrification rates of encapsulated cells under different pH conditions. The overall aim of Phase II was to assess whether cell encapsulation can provide protection to denitrifying microorganisms against low and high pH conditions.

Phase III (Batch tests using different nZVI concentrations) consists of 4 stages with the following objectives: (1) Stage III-1 (nZVI but no biomass): to examine if nitrate can be removed by the nZVI; (2) Stage III-2 (nZVI and freely suspended cells): to assess the denitrification rates of freely suspended cells under different nZVI concentrations; (3) Stage III-3 (nZVI and abiotic sodium-alginate beads): to investigate if nitrate can be removed by the nZVI and the sodium-alginate beads; (4) Stage III-4 (nZVI and encapsulated cells): to evaluate the denitrification rates of encapsulated cells under different nZVI concentrations.

Accordingly, the ability of zero-valent iron nanoparticles to enhance the ability of cell-encapsulated denitrifying microorganisms to denitrify can be assessed.

Phase IV (Batch tests using different clopyralid concentrations) includes 2 stages and the following objectives: (1) Stage IV-1 (clopyralid with freely suspended biomass): to investigate the effects on the denitrification rates of freely suspended cells under different clopyralid concentrations; (2) Stage IV-2 (clopyralid with encapsulated biomass): to assess the effects on the denitrification rates of encapsulated cells under different clopyralid concentrations. Therefore, it can be evaluated whether cell encapsulation can provide protection to denitrifying microorganisms against clopyralid.

3. Materials and methods

3.1. Synthetic wastewater and feed

Synthetic wastewater was used to keep consistency of the reactor's feed in terms of a constant COD of 168 mg/L and nitrate loading (28 mg/L). To simulate municipal wastewater, acetate (215 mg/L) was used as the carbon source with the other components (Table 3.1) dissolved in chlorine-free tap water (Aslan & Turkman, 2005, Qiu, Shi & He, 2010; Yoo et al., 1999). The optimal COD/N ratio for denitrifying bacteria has been reported to be from 5:1 to 10:1 (Nagaoka, 1999); thus, the nitrate-nitrogen concentration in the reactor was set at 28 mg/L to provide a COD/N ratio of 6:1. To maintain the nitrate-nitrogen concentration at 28 mg/L, 20 mL of 170 g/L $NaNO_3$ solution was fed into a 20 L reactor using a peristaltic pump once per cycle.

Table 3.1: Formula of Synthetic Wastewater

Nutrient	Concentration (mg/L)
CH_3COONa	215
$NaNO_3$	170
KH_2PO_4	5.41
$CaCl_2$	0.26
$NaHCO_3$	0.59
$MgSO_4{\cdot}7H_2O$	0.13
$FeSO_4{\cdot}7H_2O$	6.61
$CuSO_4{\cdot}5H_2O$	0.05
$Al_2(SO_4)_3{\cdot}16H_2O$	0.38

3.2. Bioreactor setup

Although the SBR is often used as an aerobic reactor, it can be operated in either anoxic or anaerobic conditions if the aeration period is removed. Denitrifying biomass was enriched in a 20-litre stainless steel cylinder anoxic SBR inoculated with activated sludge which was controlled and monitored by a personal computer. A submersible pump (Model 2E-38N) was used for feeding the synthetic wastewater to the SBR and a peristaltic pump (Masterflex 7553-75, 7518-00 pump head, 96410-16 tubing) was used for feeding the $NaNO_3$ solution. An oxidation-reduction potential (ORP) probe was placed in the reactor and connected to the computer for collecting ORP data. Schematic details of the anoxic SBR system are shown in

Fig 3.1 and Figure 3.2. According to Dong, Parker and Dagnew (2016), to ensure sludge production so that there are enough microorganisms for encapsulation, the hydraulic retention time (HRT) should be approximately 12 hours and the sludge retention time (SRT) should be around 40 days. The reactor was operated at ambient temperature (10-25 ^{o}C) and near-neutral pH.

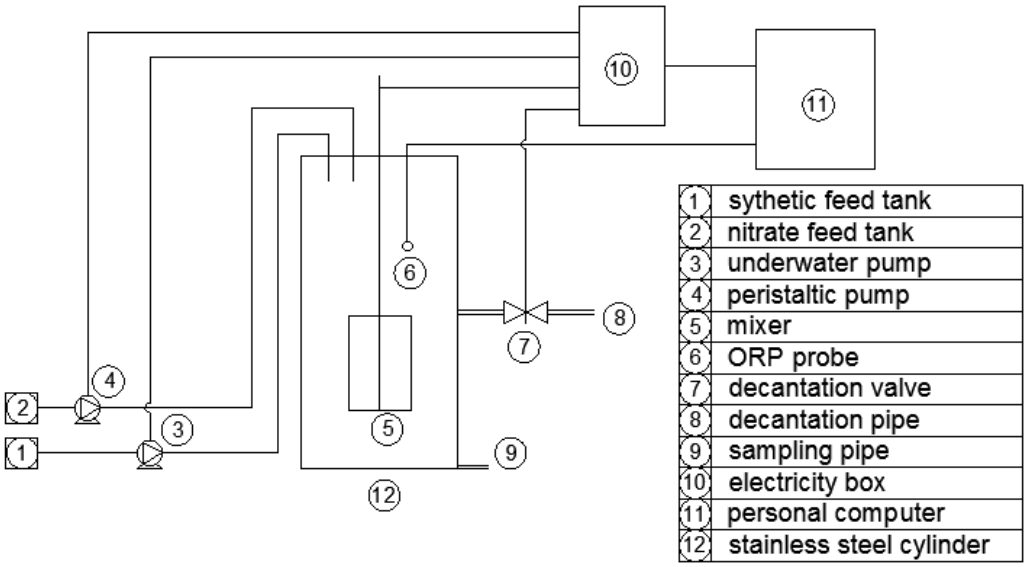

Figure 3.1: Schematic of the anoxic SBR

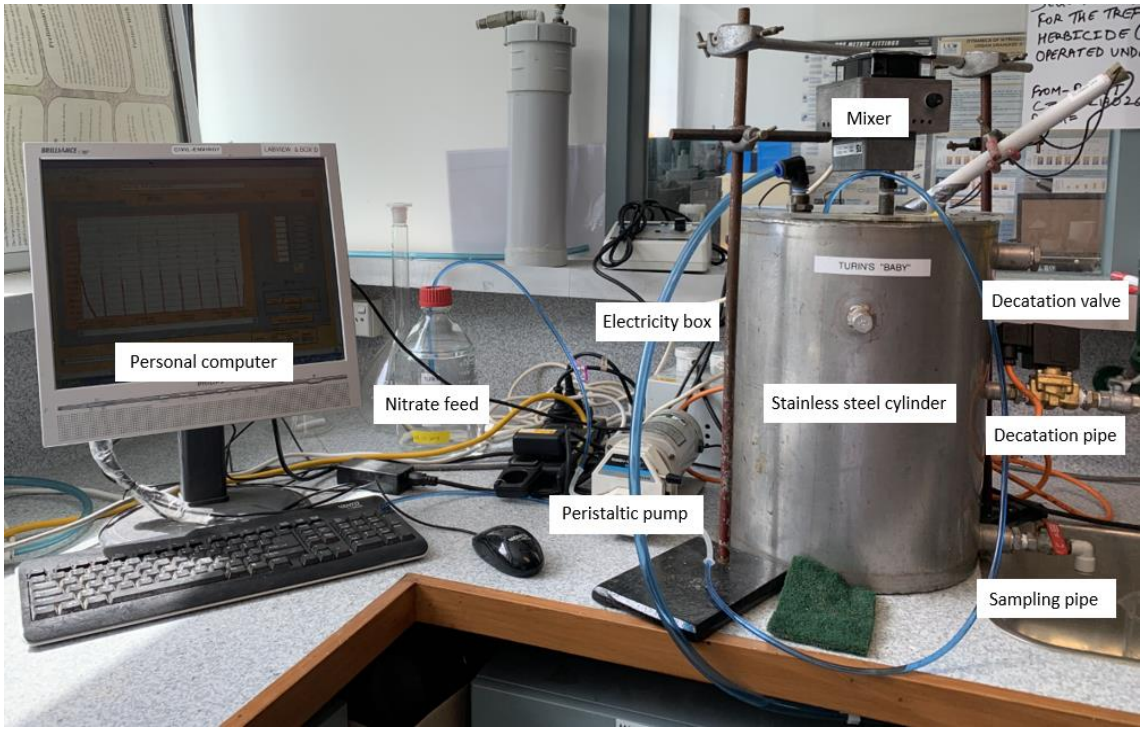

Figure 3.2: The anoxic SBR

3.3. Enrichment of denitrifying bacteria and SBR operating conditions

Activated sludge was collected either from the Christchurch Wastewater Treatment Plant (WWTP) located in the Bromley suburb of Christchurch, New Zealand or the Pines WWTP located in Rolleston, New Zealand. The sludge was washed with chlorine-free tap water 3 times a day for 3 days to remove residual COD. After washing, 10 L of the sludge was poured into the 20-L SBR which was operated under anoxic conditions (ORP between -50 and -150 mV). The sludge was then fed with 10 L synthetic wastewater and 20 mL of 170 g/L $NaNO_3$ solution and operated at a 12-hour HRT. Each anoxic SBR cycle was operated for a total time of 12 hrs with a fill period of 5 min, after which nitrate solution was added for 2 min, a mix period for 588 min, a settle period for 120 min, and a decant period for 5 min. The SRT was controlled by collecting a volume of settled sludge during the decant period (Hill & Khan, 2008). The SBR was operated for about 4 weeks for stabilisation (< 10 % variation in TSS) before the biomass was harvested for cell encapsulation.

3.4. Cell entrapment procedure

The denitrifying mixed culture was entrapped in calcium alginate according to a modified procedure adopted from van Ginkel et al. (1983). The enriched cells were harvested during the mixing phase and centrifuged at 7,000 rpm for 15 min (de-Bashan & Bashan, 2010). Sodium alginate was dissolved in de-ionised water to form a solution at a concentration of 2 % (de-Bashan & Bashan, 2010). The centrifuged cells were then added to the sodium alginate solution at a concentration of 5.69 ± 0.23 g volatile suspended solid (VSS)/L. Afterwards, the mixture was stirred at 600 rpm for 10 minutes using a magnetic stir bar to form a homogeneous suspension (de-Bashan & Bashan, 2010). The mixture was dropped from a height of approximately 10 cm into a 3.5% $CaCl_2$ solution by using a peristaltic pump (Masterflex 7553-75, 7518-00 pump head, 96410-16 tubing), to form spherical calcium alginate beads (through sodium and calcium exchange) (de-Bashan & Bashan, 2010). The beads were stirred in the 3.5 % $CaCl_2$ solution for 3 h and immediately placed in a reactor (de-Bashan & Bashan, 2010). The cell-encapsulation equipment can be seen in Figure 3.3. All entrapped beads were approximately 5 mm in diameter as shown in Figure 3.4, which is the same as the value reported by Hill & Khan (2008).

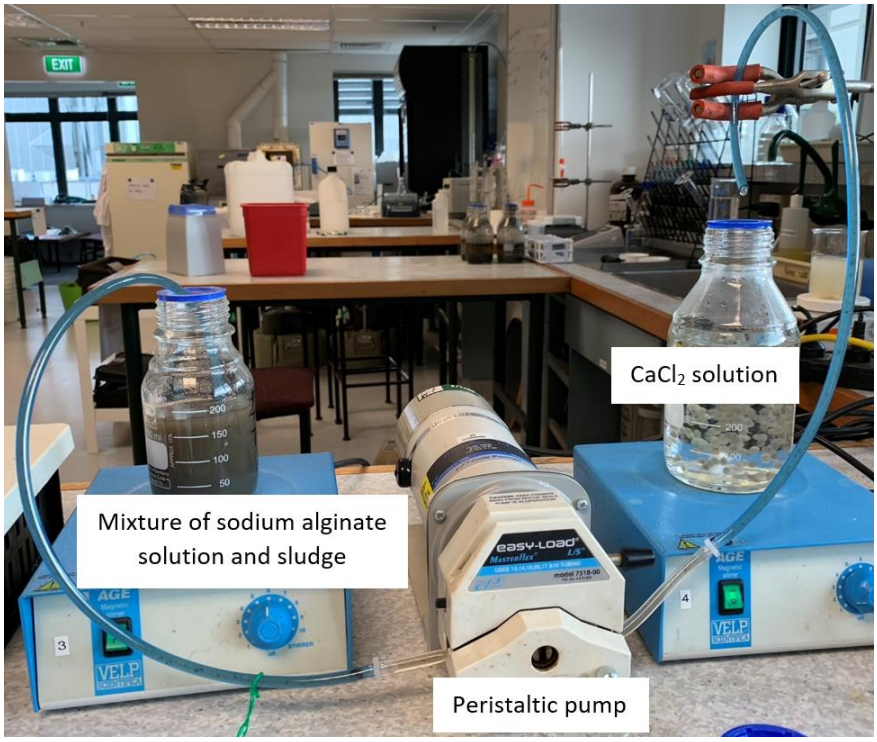

Figure 3.3: The cell-encapsulation equipment

Figure 3.4: Diameter of the beads

3.5. Denitrification tests

Batch tests were conducted to assess the denitrifying activity of the biomass under different conditions. Nitrate-nitrogen concentration was monitored over the duration of the assay. From the concentrations of nitrate at different time intervals, the denitrification rates were determined. The tests were conducted in three phases with different purposes as described in Chapter 2.7 (objectives). The pH was modified according to each experimental phase objective and varied between 5 and 9. Additionally, nanoscale ZVI particles and clopyralid were utilised to investigate their potential effect on the denitrification performance for both free and encapsulated cells.

In phase I, the operating conditions were identical to the SBR setup (HRT = 12 hours, SRT = 40 days) (Dong et al., 2016; Huang et al., 2011). The concentration of biomass was maintained around 4500 mg/L as total suspended solid (TSS). After the biomass concentration stabilised, several parameters (i.e. NO_3-N, COD, ORP) were monitored to determine whether the microorganisms were healthy enough to yield a reasonable denitrification rate (0.12 mg N/(g VSS·min))(Fernandez-Nava, Maranon, Soons & Castrillon, 2008).

The Phase II had three stages: (1) Stage II-1 containing freely suspended cells, (2) Stage II-2 containing sodium-alginate beads and no biomass (abiotic conditions) and (3) Stage II-3 containing encapsulated cells. In Stage II-1, denitrifying activity tests were conducted in 3 separate 1-litre batch reactors. The contents of the reactors were mixed during the tests using a magnetic stirrer. The concentration of biomass in these reactors was about 4500 mg TSS/L, and the batch reactors were fed with 246 mg sodium acetate and 0.10 mL 170 g/L $NaNO_3$. At the same time, the pH was modified and controlled at a pH of 5, 7, and 9 respectively by adding the pH buffers listed in Table 3.2. The same feed and pH buffers were used in the Stage II-2 and Stage II-3 tests.

In Phase III, there were 4 stages: (1) Stage III-1 (nZVI but no biomass), (2) Stage III-2 (nZVI and freely suspended cells), (3) Stage III-3 (nZVI and abiotic sodium-alginate beads) and (4) Stage III-4 (nZVI and encapsulated cells). For all stages, the concentrations of sodium acetate and sodium nitrate were the same as in Phase II. For each stage, two separate 1-litre batch reactors were operated at the same time using 0.5 g/L and 3 g/L nZVI respectively. To prevent any potential interference caused by the magnetic stirrer, mixing was done using an orbital scrolling shaker.

Table 3.2: Composition of pH buffers used in batch tests (McIlvaine, 1921; Cao, et al., 2013)

pH	Chemical & concentration
5.0	Na_2HPO_4: 14.6 g/L, Citric acid: 9.3 g/L
7.0	Na_2HPO_4: 23.39 g/L, Citric acid: 3.39 g/L
9.0	$Na_2B_4O_7$: 3.8 g/L

In Phase IV, there were 2 stages: (1) Stage IV-1 (clopyralid with freely suspended biomass), (2) Stage IV-2 (clopyralid with encapsulated biomass). For both stages, the concentrations of sodium acetate and sodium nitrate were the same as Phase II. For each stage, two separate 1-litre batch reactors were operated at the same time using 50 mg/L and 300 mg/L clopyralid respectively.

3.6. Analytical methods

For the SBRs, samples were taken hourly for the first 5 hours of each operating cycle from each reactor, centrifuged and filtered before being preserved and tested for COD, nitrate and nitrite. Preservation of the samples was done by adding 1-2 drops of sulphuric acid to reduce the pH to < 2. The samples were then stored at 4 ^{o}C for no more than 3 days. During the batch tests, nitrate-nitrogen concentrations were sampled and measured every 10 minutes in the first hour and every 15 minutes in the following hours as necessary. To measure NO_3-N and COD, the colorimetric methods described in the Standard Methods for the Examination of Water & Wastewater by Eaton, Clesceri, Greenberg, & Franson (2005) were followed.

4. Result and discussion

4.1. Phase I: Preliminary tests

4.1.1. SBR operation and biomass-enrichment

Since the main purpose of the SBR was to be a sludge generator for subsequent batch tests, the concentration of total suspended solid (TSS) was monitored to see if the biomass concentration was being enriched in the reactor. The TSS results with time are plotted in Figure 4.1. As can be seen, the initial TSS was approximately 1600 mg/L; and, after a steady growth for about 40 days, the biomass concentration stabilised around 4600 ± 455 mg/L as TSS, which is only a little higher than the concentration of 3200 mg/L as VSS reported by Hill & Khan (2008) for encapsulation. After the biomass concentration started to plateau, the denitrification efficiency was checked to see if the sludge had an adequate nitrate removal capability. During the plateau period, 500 mL of sludge was wasted daily for sampling purposes and to ensure a 40-day sludge retention time (SRT).

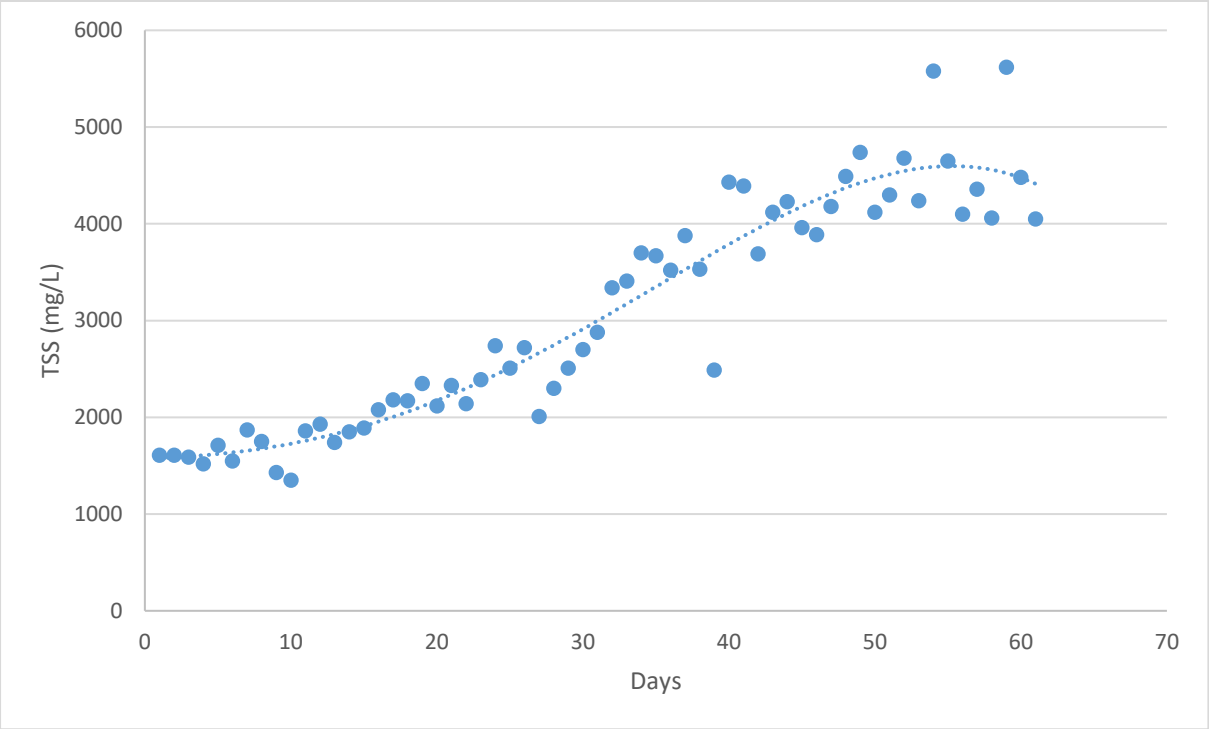

Figure 4.1: Profile of TSS in the SBR

4.1.2. Denitrification performance check

The denitrification performance of the SBR sludge was assessed at the start of the mixing phase in each cycle. The initial concentration of nitrates was around 28 mg/L and the change in NO_3-N concentration with time for these tests are plotted in Figure 4.2. The error bars indicate the standard deviation of the experimental results from three replicates. Figure 4.2 indicates that approximately 97 % of nitrates was removed in 50 minutes. A spike (28.48 ±

0.47 mg N/L) was observed at the 20-minute mark in all 3 cases; however, since this in essence amounted to the creation of nitrates, it was prudent to ignore this measurement when calculating rates. In addition, since this spike appeared to occur in all 3 replicates, it is probable there was a systematic error. Accordingly, the zero-order reaction rate constant and the biomass-specific denitrification rate in the reactor were 0.53 mg N/min and 0.115 mg N/(g TSS·min), respectively. The denitrification rate is close to the nitrate-removal rate of biomass from a WWTP treating domestic wastewater, which was 0.12 mg N/(g VSS·min), as reported by Fernandez-Nava, Maranon, Soons & Castrillon (2008).

To test if the denitrification rates between the 20-L SBR and 500-mL batch reactors were similar; batch tests using sludge from the SBR were conducted and the results are plotted in Figure 4.3. The error bars indicate the standard deviation of the experimental results of 3 replications. In Figure 4.3, a spike also can be seen; however, the spike was at 10 minutes instead of at 20 minutes and relatively small as compared to the initial concentration (31.17 ± 3.10 mg N/L). Approximately 89 % of the nitrate was removed in the first 40 minutes. Furthermore, the reaction rate constant and the biomass-specific denitrification rate were found to be 0.65 mg N/min and 0.141 mg N/(g TSS·min), respectively. The denitrification rate appeared to be slightly higher but not dissimilar than the rate from the SBR.

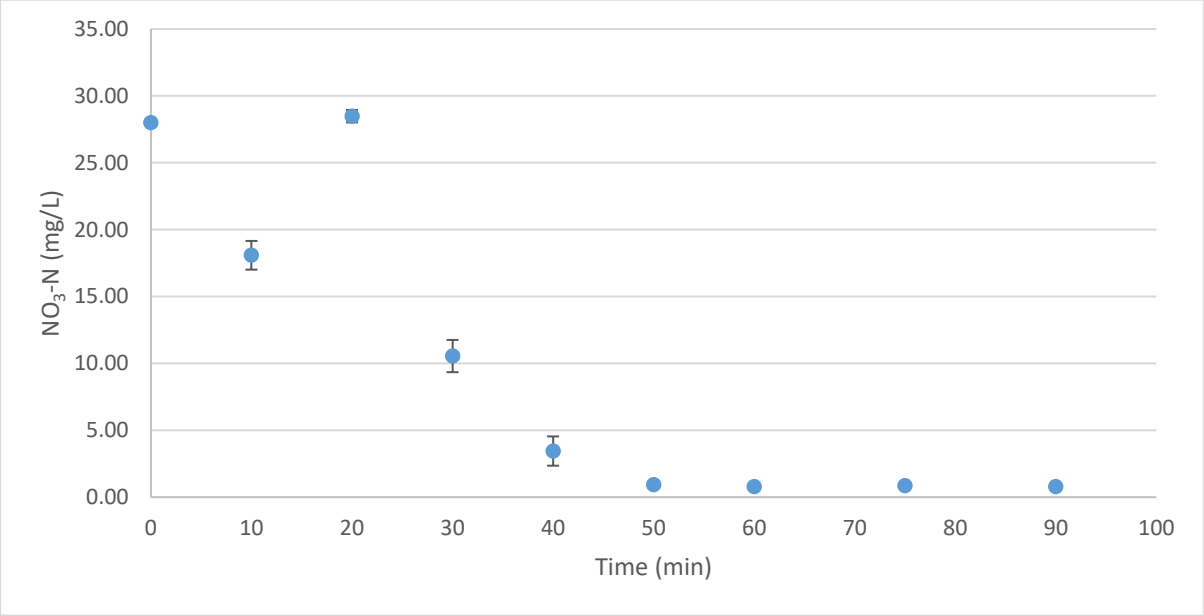

Figure 4.2: NO_3-N concentration changes with time in the SBR (n=5)

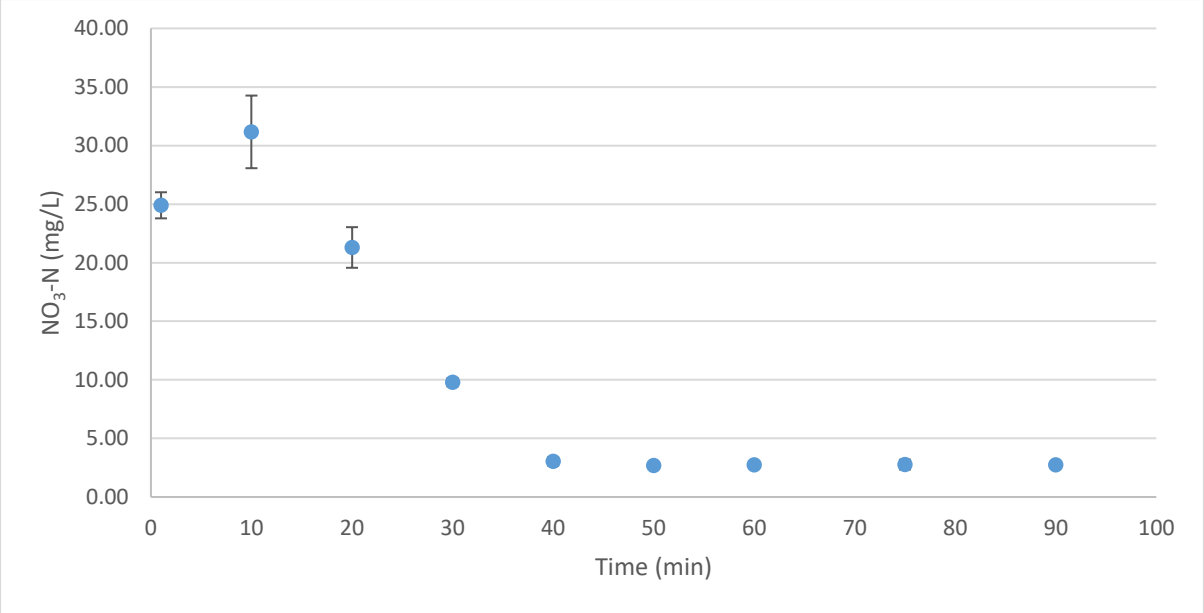

Figure 4.3: Results of the 500-mL denitrification batch tests using sludge from SBR (n=3)

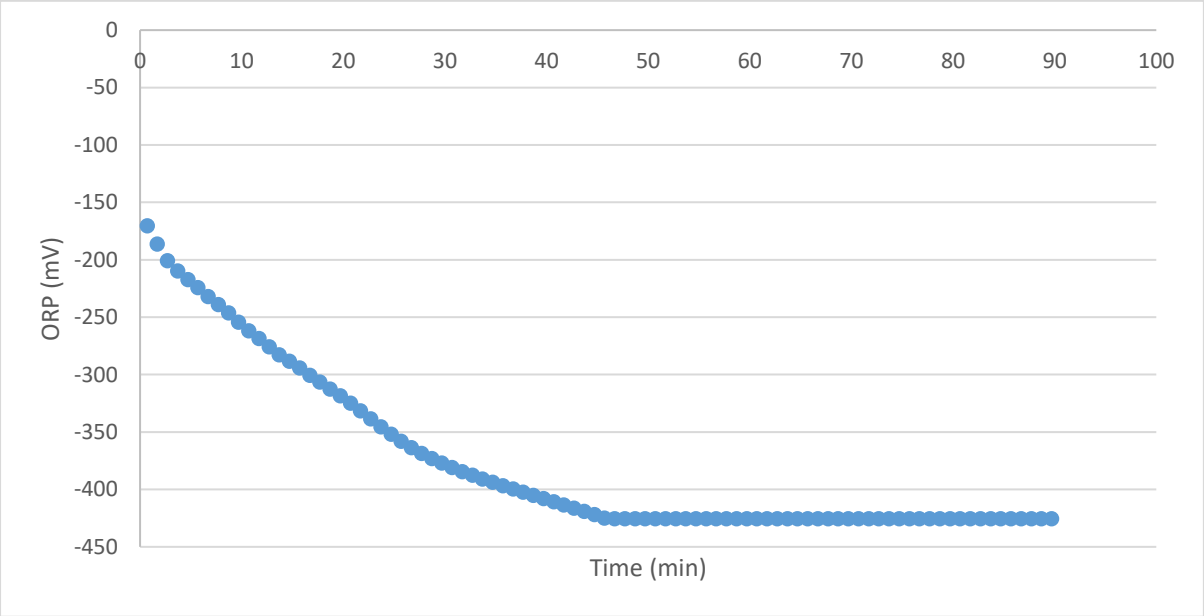

Figure 4.4: Profile of ORP in the SBR

It was also noticed that the ORP in the SBR was regularly in the -300 mV range (i.e. Figure 4.4). This indicated that the sludge was mostly anaerobic and therefore not really suitable for denitrification purposes in the long term. Correspondingly, and because of the spikes observed in both sets of denitrification tests, it was decided to test the suitability of utilising sludge from the Pines WWTP located in Rolleston, New Zealand for the batch tests since this plant was known to be a denitrifying plant and it was proven problematic to continuously enrich for denitrifying bacteria from a non-denitrifying plant (i.e. the Bromley WWTP).

Batch tests were conducted to investigate the denitrification rates using sludge from the Pines WWTP and the NO_3-N concentrations are plotted in Figure 4.5. The error bars indicate the standard deviation of the experimental results of 5 replicates. As can be seen, the nitrate removal was approximately 88 % in 40 minutes, which was close to the percent removal found in the batch tests using the SBR biomass (Figure 4.3). The reaction rate constant and the biomass-specific denitrification rate were found to be 0.65 mg N/min and 0.114 mg N/(g VSS·min), respectively. The denitrification rate appeared to be very close to the rate of the SBR and slightly lower than the rate of the batch tests using sludge from the SBR. Additionally, no spike was observed in the tests using sludge from Pines WWTP. Thus, it was decided that sludge from the Pines WWTP was to be collected and utilised for the next set of tests (Phase II, III and IV).

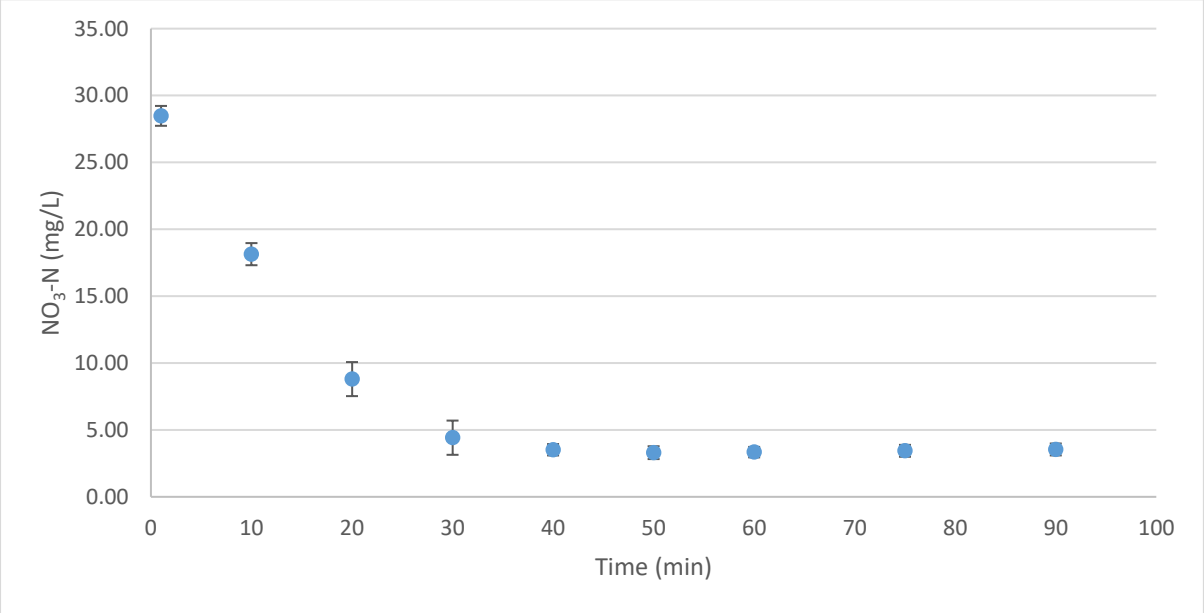

Figure 4.5: Results of the denitrification batch tests using sludge from Pines WWTP (n=5)

4.2. Phase II: Denitrification Rates Under Different pH Conditions

4.2.1. Stage II-1: Batch tests using freely suspended cells

The influence of pH on the nitrate-removal rate was assessed via batch tests. Three pH ranges were targeted using pH buffers of 5.02 ± 0.02, 7.03 ± 0.48, and 9.33 ± 0.03, respectively. After 90 to 120-minute testing, the pH in the reactors stayed at the original value suggesting that the pH buffers were maintaining the targeted pH.

The initial concentration of nitrates was around 28 mg/L and the change of NO_3-N concentration with time for these tests are plotted in Figure 4.6. The error bars indicate the standard deviation of the experiment results of at least 3 replications for each pH condition. For all profiles, nitrate removal was in the range of 86 - 88 % indicating a healthy sludge well-suited for the removal of nitrates. Along with the measured VSS of the sludge, these results were used to determine biomass-specific denitrification rates. Before computing the biomass-specific denitrification rates (as well as the reaction rate constants), the proper reaction order/model was determined by comparing the regression values from potential models. For these results, zero-order (linear) and first-order (exponential) models were compared. When the NO_3-N values effectively plateaued, they were not considered for zero-order modelling.

For the neutral-pH graph (i.e. Figure 4.6 (a)), the R^2 values for the linear and exponential models were 0.91 and 0.95, which suggests the exponential model is a better fit to the NO_3-N decay. This was also true for the low and high-pH data with the R^2 values of the exponential models in these two cases being 0.99 and 0.98, respectively. However, the regression values for the linear models of neutral, low and high pH cases were 0.91, 0.93 and 0.96, which are also good for describing the denitrification trend. As such, zero-order models can be utilised to describe the decay in all 3 cases and this order of model was used to determine the reaction rate constants and the biomass-specific denitrification rates.

The zero-order reaction rate constants were found to be 0.64 mg N/min, 0.36 mg N/min, and 0.30 mg N/min respectively for the neutral, low and high pH data. The biomass-specific denitrification rates were also calculated to be 0.113, 0.063 and 0.053 mg N/(g VSS·min), respectively. As can be seen, at the low pH, the denitrification rate was slightly higher than half the rate under neutral pH condition, while at the high pH, the rate was lower than the low pH rate being approximately half the neutral pH rate. These results suggest that the denitrification performance for freely suspended cells was negatively affected at both high and low pH values, with the high pH appearing to have a marginally greater impact on the NO_3-N removal rate.

The neutral pH denitrification rate of 0.113 mg N/(g VSS·min), is close to the nitrate-removal rate of biomass from a wastewater treatment plant located in Spain, which is 0.12 mg N/(g VSS·min), as reported by Fernandez-Nava, Maranon, Soons & Castrillon (2008).

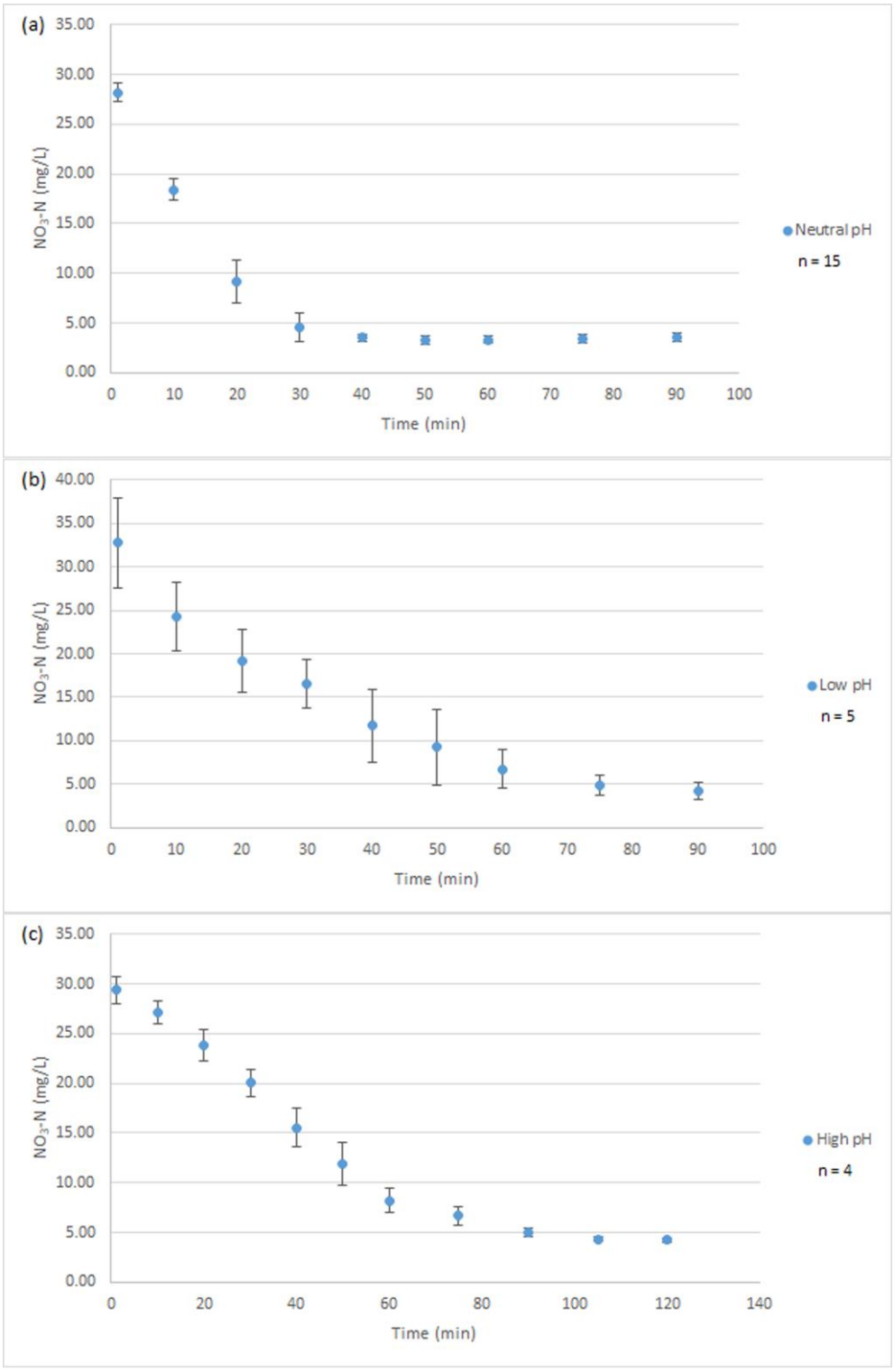

Figure 4.6: Results of batch tests with freely suspended cells under different pH conditions

4.2.2. Stage II-2: Abiotic tests

Before checking the denitrification rates associated with the encapsulated cells, the baseline condition should be assessed to determine if there was any potential adsorption or chemical bonding of the nitrate by the sodium-alginate beads. The results from the abiotic tests (i.e. addition of nitrate to sodium-alginate beads without biomass) are plotted in Figure 4.7. As can be seen, at all three pH values, the NO_3-N concentrations dropped instantly from 28 mg N/L after adding the nitrate solution to 18.52 ± 0.52, 1.29 ± 0.16 and 14.26 ± 0.99 mg N/L for the neutral, low and high pHs, respectively. This means that 48.8% - 92.5% of the initial nitrate was instantly taken up by the cell encapsulation material (sodium alginate), which suggests either some kind of adsorption reaction or some kind of chemical reaction between the nitrates and the sodium alginate. This is further explored in the next section.

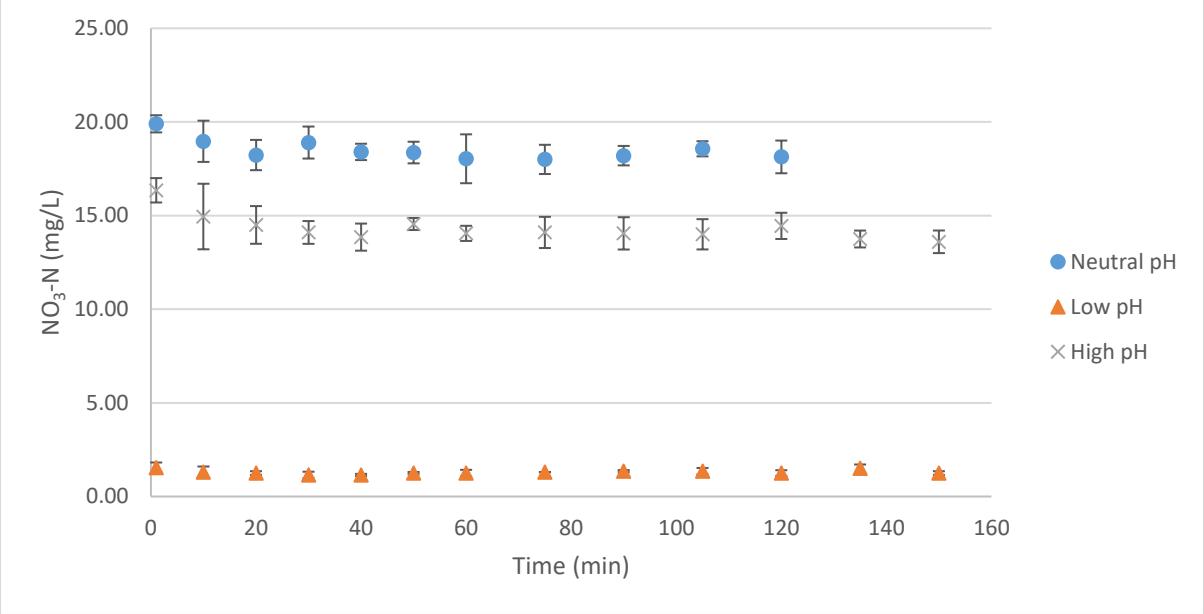

Figure 4.7: Results of abiotic tests with sodium-alginate beads under different pH conditions

4.2.3. Stage II-3: Batch tests using encapsulated cells

Batch tests were then conducted to investigate the denitrification rates using encapsulated cells, again under different pH conditions. The pH ranges were adjusted with the same pH buffers as for the free-cell tests. The buffers showed great efficiency in maintaining the pH at 4.79 ± 0.23 and 6.77 ± 0.35; however, the high-pH buffer only managed to adjust the pH to 6.62 ± 0.41. Obviously, something associated with the encapsulation method interfered with the ability of the buffer to push the pH up to the equivalent value associated with the free cells. Since further additions of buffer solution would dilute the initial nitrate concentration, a decision was made to continue with the high-pH test acknowledging the different high pH starting conditions between the free and encapsulated cells. That is the so-called high-pH condition was effectively a near-neutral-pH condition.

The NO_3-N concentrations for these tests are plotted in Figure 4.8. For all profiles, nitrate removal was approximately 95 % indicating that the encapsulated cells were also able to remove the nitrates. As can be seen in Figure 4.8, the NO_3-N concentration dropped instantly after the addition of the nitrate feed which had been targeted to provide an initial concentration of about 28 mg/L (i.e. the same starting conditions as the free cell situation). However, as can be seen in Figure 4.8, the initial target concentration of 28 mg/L was not reached in any of the pH conditions.

After the initial drop at time zero, the nitrate-nitrogen concentrations gradually climbed for at least 60 minutes in the two near-neutral pH conditions before decreasing rapidly (Figure 4.8 (a) and (c)). However, as mentioned, this decrease did not occur under low-pH conditions. In the latter case, the NO_3-N slowly increased from 2 to 12 mg/L in the first 135 minutes; eventually plateauing, which suggests that the encapsulated denitrifying biomass were completely deactivated at the low pH. From the results, it appears that either something that is a function of the encapsulation mechanism releases nitrate (i.e. something related to the sodium alginate) or something related to bacterial release of nitrates is occurring. It is noted that the final nitrate concentration in the low-pH reactor did not return to 28 mg/L; however, it did closely reach the initial starting nitrate concentration associated with the neutral-pH reactor. This means that whatever reaction is occurring between the nitrate and the sodium alginate (i.e. adsorption or chemical bonding) is to some extent reversible (i.e. desorption or dissolution of the chemical bond). Since the low-pH profile was uncharacteristic, kinetic analyses were only conducted for the neutral and “high” pH results.

As was the case for the free-cell conditions, zero-order models were used to describe the decay in both the neutral and “high” pH cases with this model used to determine the reaction rate constants and the biomass-specific denitrification rates. Accordingly, it should be noted that NO_3-N values showing an increasing trend were not considered in the calculation of the biomass-specific denitrification rates (i.e. the first part of Figure 5.2.3 (a) and (c) and all of 5.2.3 (b)).

The zero-order reaction rate constants were found to be 0.41 mg N/min and 0.19 mg N/min respectively for the neutral and high pH data; while the biomass-specific denitrification rates were calculated to be 0.072 and 0.033 mg N/(g VSS·min). As can be seen, at the so-called high pH, the denitrification rate was slightly lower than half the rate under neutral pH condition, which was the same ratio as found by the results of the freely suspended cells. Additionally, in both neutral and high pH cases, the denitrification rates of the encapsulated cells were approximately 2/3 of the rates of freely suspended cells. These results suggest that for this research cell-encapsulation technology negatively affected the denitrification rates (under all pH conditions), instead of enhancing nitrate-removal performances as had been previously reported (Mallick, 2002).

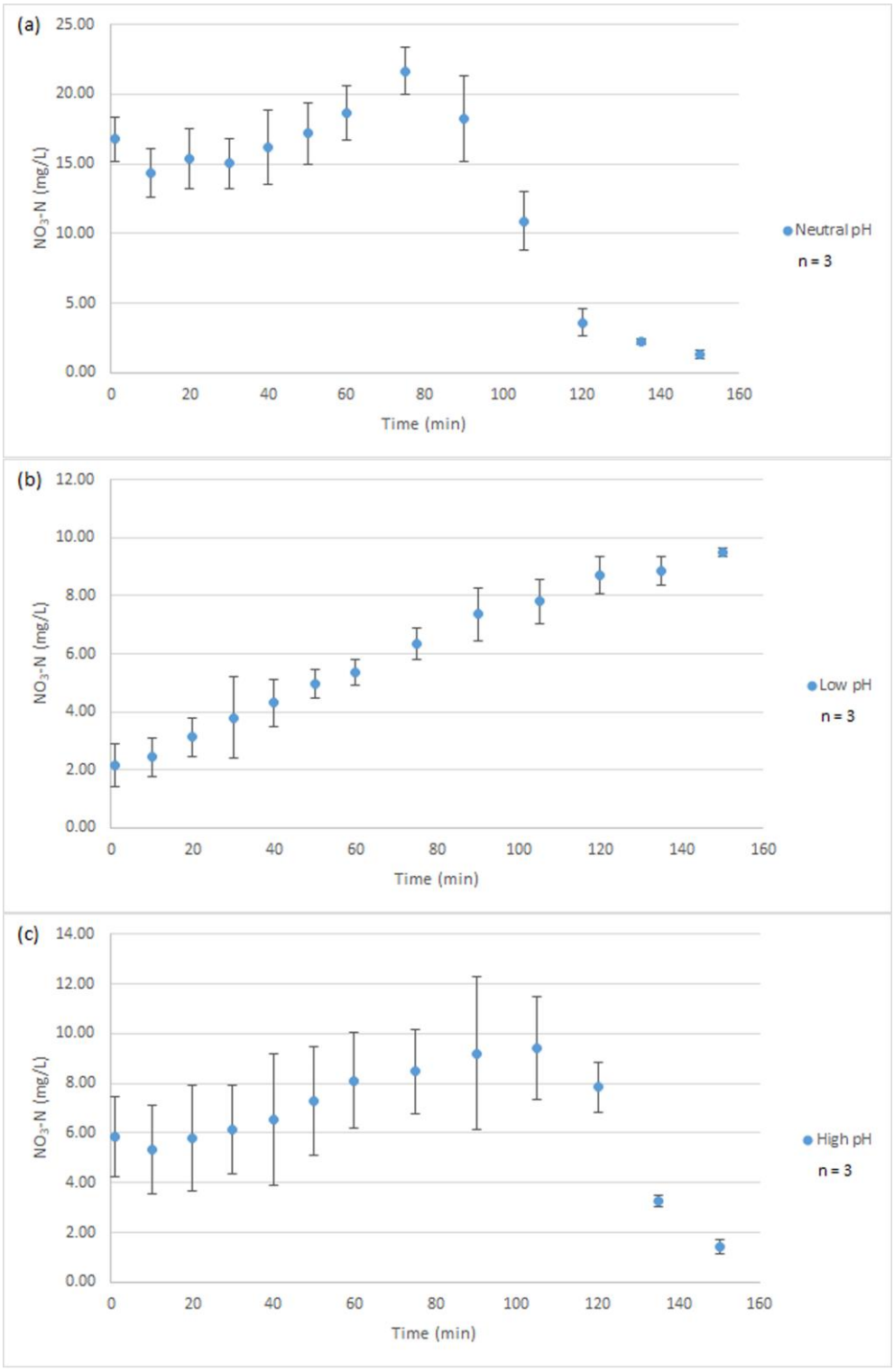

Figure 4.8: Results of batch tests with encapsulated cells under different pH conditions

4.3. *Phase III: Denitrification Rates under Different nZVI Concentrations*

4.3.1. Stage III-1: Baseline tests

Before checking the denitrification rates associated with the nanoparticles, the baseline condition should be assessed to determine if there was any potential removal of the nitrate caused by chemical reactions with nZVI. The results from the preliminary tests (i.e. addition of nZVI to the synthetic feed with a nitrate concentration of 28 mg N/L) are plotted in Figure 4.9. As can be seen, the NO_3-N concentrations stabilised around 28.36 ± 0.30 mg N/L and 28.50 ± 0.57 mg N/L respectively for 0.5 and 3 g/L nZVI, indicating no nitrate was removed by chemical reactions with nZVI in both cases. This means the nitrate-removal rates obtained in the following batch tests using freely suspended cells should be the biological denitrification rates.

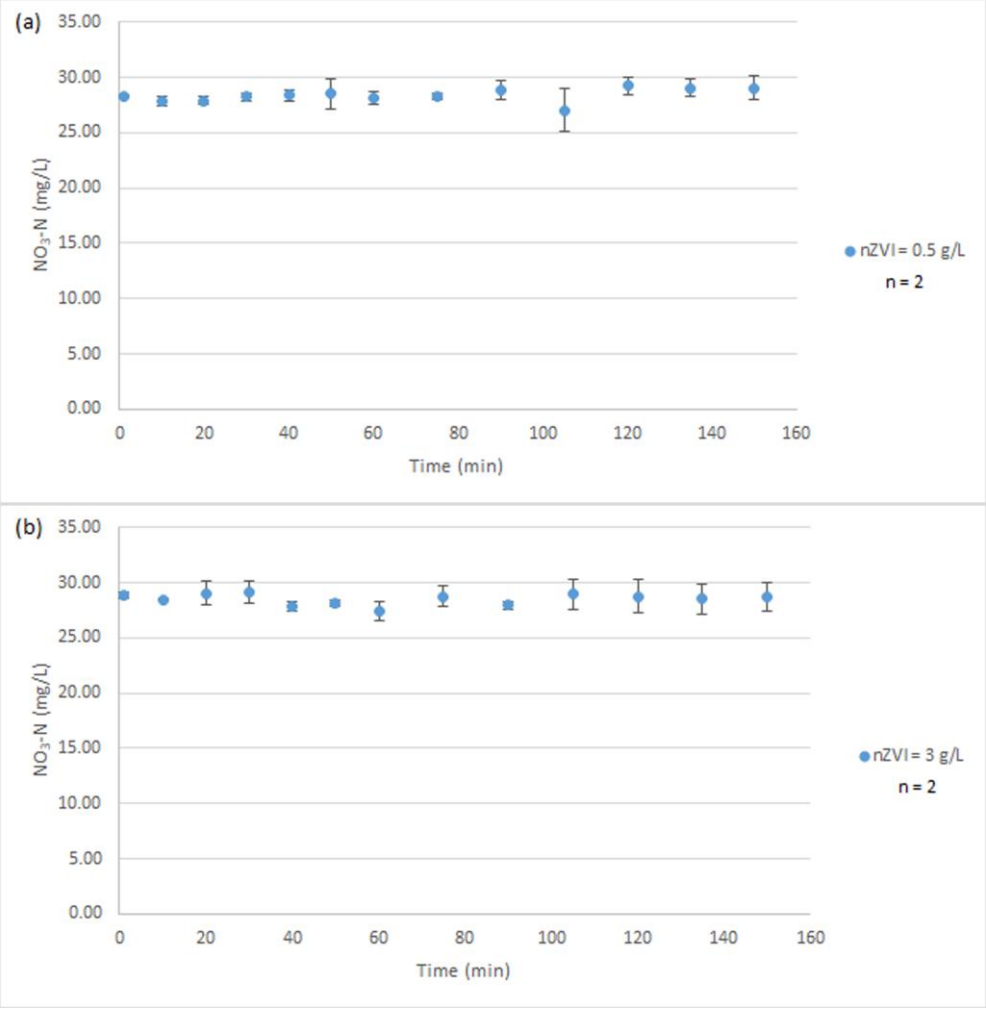

Figure 4.9: Results of batch tests under different nZVI concentrations without biomass

4.3.2. Stage III-2: Batch tests using freely suspended cells

The results from the batch tests using different nZVI concentrations (0.5 and 3 g/L) are plotted in Figure 4.10 (b) & (c). As can be seen, under both conditions, nitrate removal was in the range of 70 - 78 % indicating denitrification proceeded readily; however, the removal was not as large as that of the case without addition of nZVI (88% removal efficiency, Figure 4.10 (a)). Denitrification rates were only calculated for the declining portion of the data; that is to say, when observable denitrification activity occurred. Moreover, the error bars in Figure 4.10 indicate the standard deviation of the three replicates for each nZVI concentration appear to be relatively small during the decreasing phase (generally from 30 to 90 minutes). This suggests denitrification rates can best be determined during this period. Along with the measured VSS of the sludge, these results were used to determine the biomass-specific denitrification rates.

Also shown in Figure 4.10 (b) & (c), is the fact that the NO_3-N concentration dropped instantly after the addition of the nitrate feed from a target of about 28 mg/L (i.e. the same starting conditions as the cases without nZVI (Figure 4.10 (a)). This means that approximately 27% of the initial nitrate was removed immediately by the nanoparticles, which surprisingly seems to contradict in the baseline tests shown in Figure 4.9.

To keep consistency with Section 4.2, zero-order model was employed to describe the decay observed in Figure 4.10 (b) & (c). The zero-order reaction rate constants were found to be 0.14 mg N/min and 0.13 mg N/min respectively for the 0.5 and 3 g/L nZVI data; while the biomass-specific denitrification rates were calculated to be 0.025 and 0.022 mg N/(g VSS·min). The rates are so close together that is suggested that there is no difference found between the 0.5 and 3 mg/L nZVI cases. However, comparing these rates to the case without addition of nZVI (0.113 mg N/(g VSS·min))(Figure 4.10 (a)); it appears that the nitrate-removal rates were severely impacted by the addition of nanoparticles.

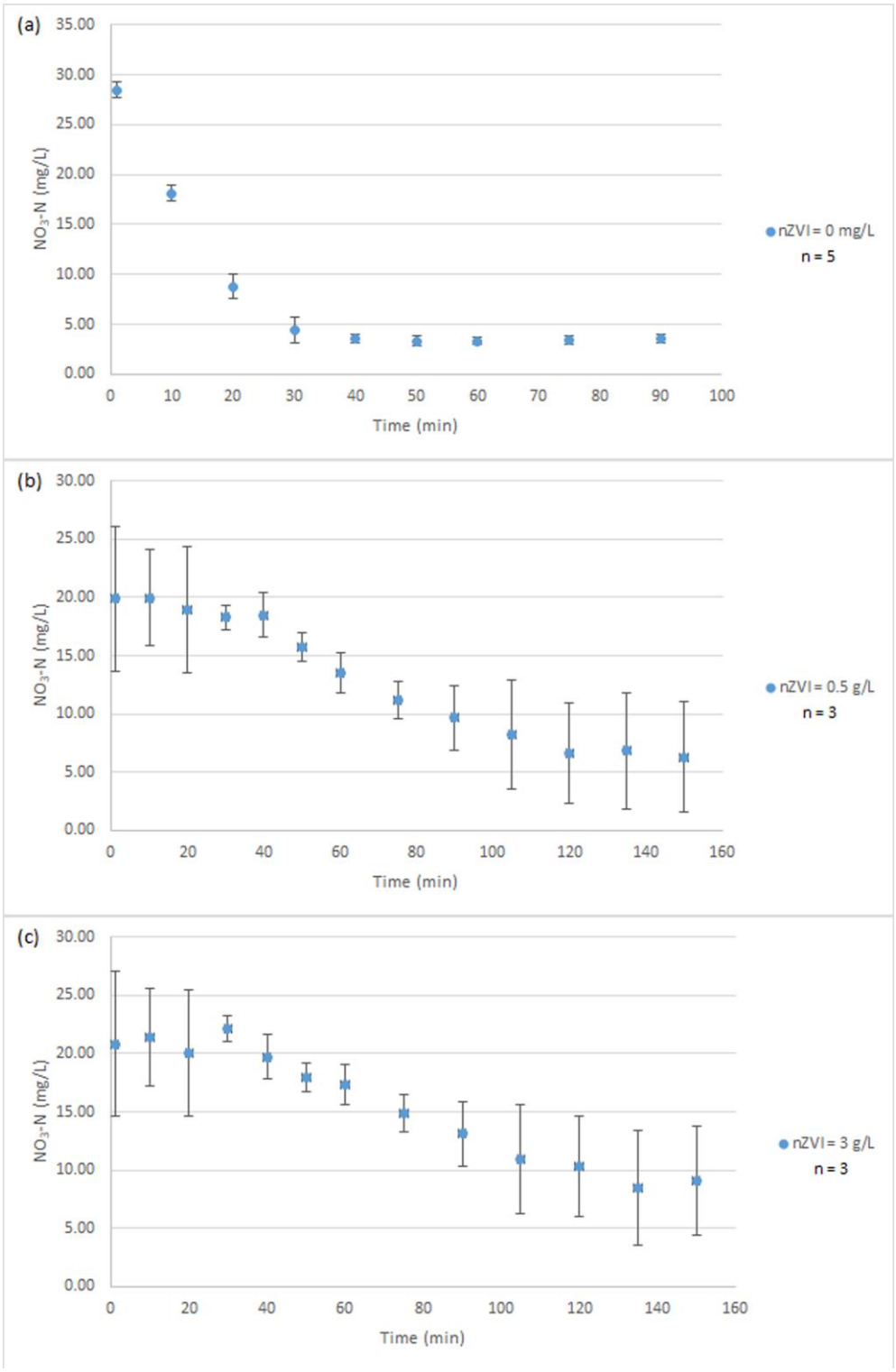

Figure 4.10: Results of batch tests with freely suspended cells under different nZVI concentrations

4.3.3. Stage III-3: Batch tests using abiotic alginate beads

Before checking the denitrification rates associated with the nanoparticles and encapsulated cells, the baseline condition were assessed to determine if there was any potential removal of the nitrate by the sodium-alginate beads and the nZVI. The results from the abiotic tests (i.e. addition of nZVI to batch reactors with synthetic feed and sodium-alginate beads without biomass) are plotted in Figure 4.11. As can be seen, the NO_3-N concentrations stabilised around 26.39 ± 0.24 mg N/L and 26.74 ± 0.96 mg N/L respectively for 0.5 and 3 g/L nZVI. Since the nitrate concentrations in both cases were close to the targeted initial nitrate concentration (28 mg N/L), there was either minor or no nitrate removal by the sodium-alginate beads and the nZVI. This means the nitrate-removal rates obtained in the following batch tests using encapsulated biomass should be the biological denitrification rates.

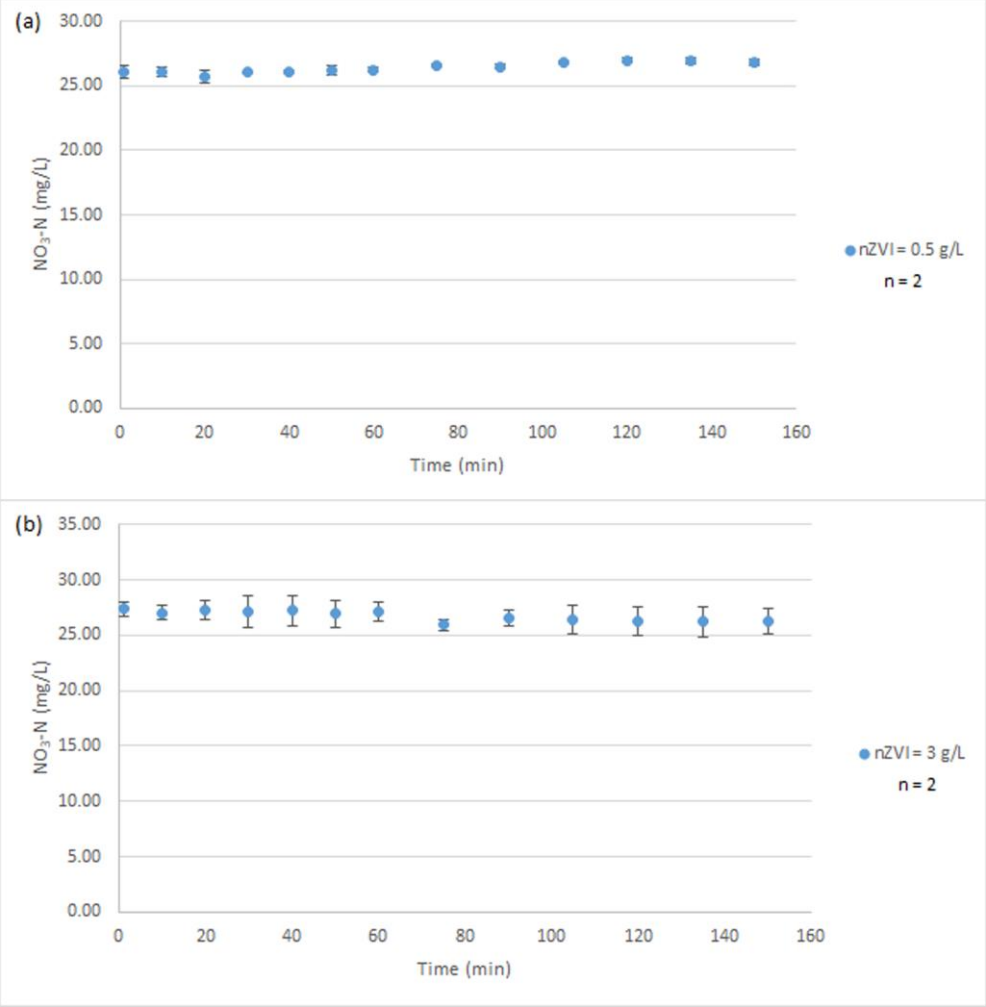

Figure 4.11: Results of batch tests with blank sodium-alginate beads under different nZVI concentrations

4.3.4. Stage III-4: Batch tests using encapsulated cells

Batch tests were then done using encapsulated cells under different nZVI concentrations (0.5 and 3 g/L) to investigate the denitrification rates. The results of these tests were plotted in Figure 4.12 (b) & (c). As can be seen, in these two cases, nitrate removals were approximately 46% and 23%, respectively under 0.5 and 3 g/L nZVI. This indicates that the encapsulated cells were also able to remove the nitrates, however, the removal efficiency was not as high as the case without addition of nanoparticles (95%). As shown in Figure 4.12, the NO_3-N concentration dropped instantly to approximately 25 mg/L after the addition of the nitrate feed which had been targeted to provide an initial concentration of about 28 mg/L (i.e. the same starting conditions as the free cell cases). However, because the error bars encapsulate a value close to 28 mg/L, this drop may be more appearance than reality. In any case, the initial drop observed in these two cases (Figure 4.12 (b) & (c)) appeared to be substantially less than the non-nanoparticle case (Figure 4.12 (a)).

After time zero, the nitrate-nitrogen concentrations gradually climbed in the control test (Figure 4.12 (a)); however, this trend was not observed in the 0.5 g/L nZVI case. Instead, a slight but continuous decrease of NO_3-N was noted through the entire 210-min test under 0.5 g/L nZVI conditions (Figure 4.12 (b)). Meanwhile, in the 3 g/L nZVI case, due to the relatively large standard deviations, what happened after the initial drop at time zero was difficult to ascertain; however, the mean values, indicate a marginal decrease of NO_3-N from 75 to 150 minutes, but the large standard deviation of the data does not allow the calculation of a denitrification rate (Figure 4.12 (c)).

To ensure consistency with previous discussions, zero-order models were employed to describe the decay observed in Figure 4.12 (b). The zero-order reaction rate constant was 0.039 mg N/min for the 0.5 nZVI data; while the biomass-specific denitrification rate was calculated to be 0.007 mg N/(g VSS·min). This denitrification rate was lower than the rates found in the free-cell cases (Figure 4.10 (b) & (c)). For the encapsulated cells, the denitrification rate of the 0.5 g/L nZVI case was severely affected by cell encapsulation in the presence of nanoparticles being substantially less than the rate obtained with no nZVI particles (0.072 mg N/(g VSS·min)).

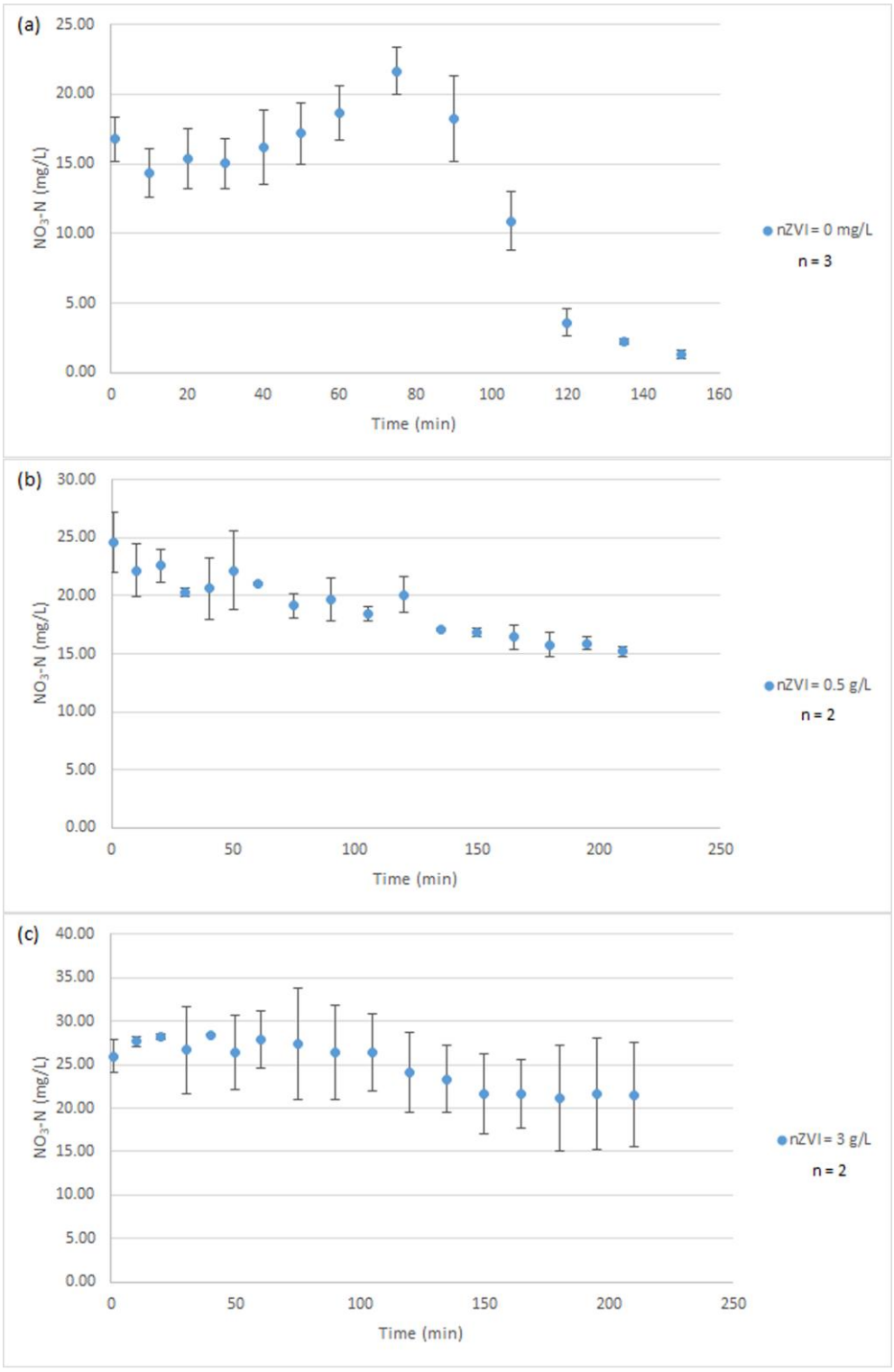

Figure 4.12: Results of batch tests with encapsulated cells under different nZVI concentrations

4.4. Phase IV: Denitrification Rates under Different Clopyralid Concentrations

4.4.1. Stage IV-1: Batch tests using freely suspended cells

The results from the batch tests using different clopyralid concentrations (50 and 300 mg/L) are plotted in Figure 4.13 (b) & (c). As can be seen, in these two cases, nitrate removals were approximately 73 % and 29 %, respectively under 50 and 300 mg/L clopyralid, indicating denitrification did happen. However, the removal percentages under both conditions were not as large as that of the case without addition of clopyralid (88% removal efficiency, Figure 4.13 (a)). The error bars in Figure 4.13 indicate the standard deviation of the replicates for each clopyralid concentration, which appears to be close to the mean values. Along with the measured VSS of the sludge, these results were used to determine the biomass-specific denitrification rates.

To keep consistency with previous chapters, a zero-order model was used to describe the decay of NO_3-N concentration observed in Figure 4.13 (b) & (c). The zero-order reaction rate constants were found to be 0.16 mg N/min and 0.06 mg N/min respectively for the 50 and 300 mg/L NZVI data; while the biomass-specific denitrification rates were calculated to be 0.027 and 0.010 mg N/(g VSS·min). Comparing these rates to the case without addition of clopyralid (0.113 mg N/(g VSS·min))(Figure 4.13 (a)); at the low clopyralid concentration, the denitrification rate was about 1/4 the rate under no clopyralid addition, while at the high clopyralid concentration, the rate was lower than the low-clopyralid rate being approximately 1/11 the zero-clopyralid rate. These results suggest that the denitrification performance of freely suspended cells was negatively affected at both high and low clopyralid concentrations, with 300 mg/L clopyralid appearing to have a greater impact on the NO_3-N removal rate.

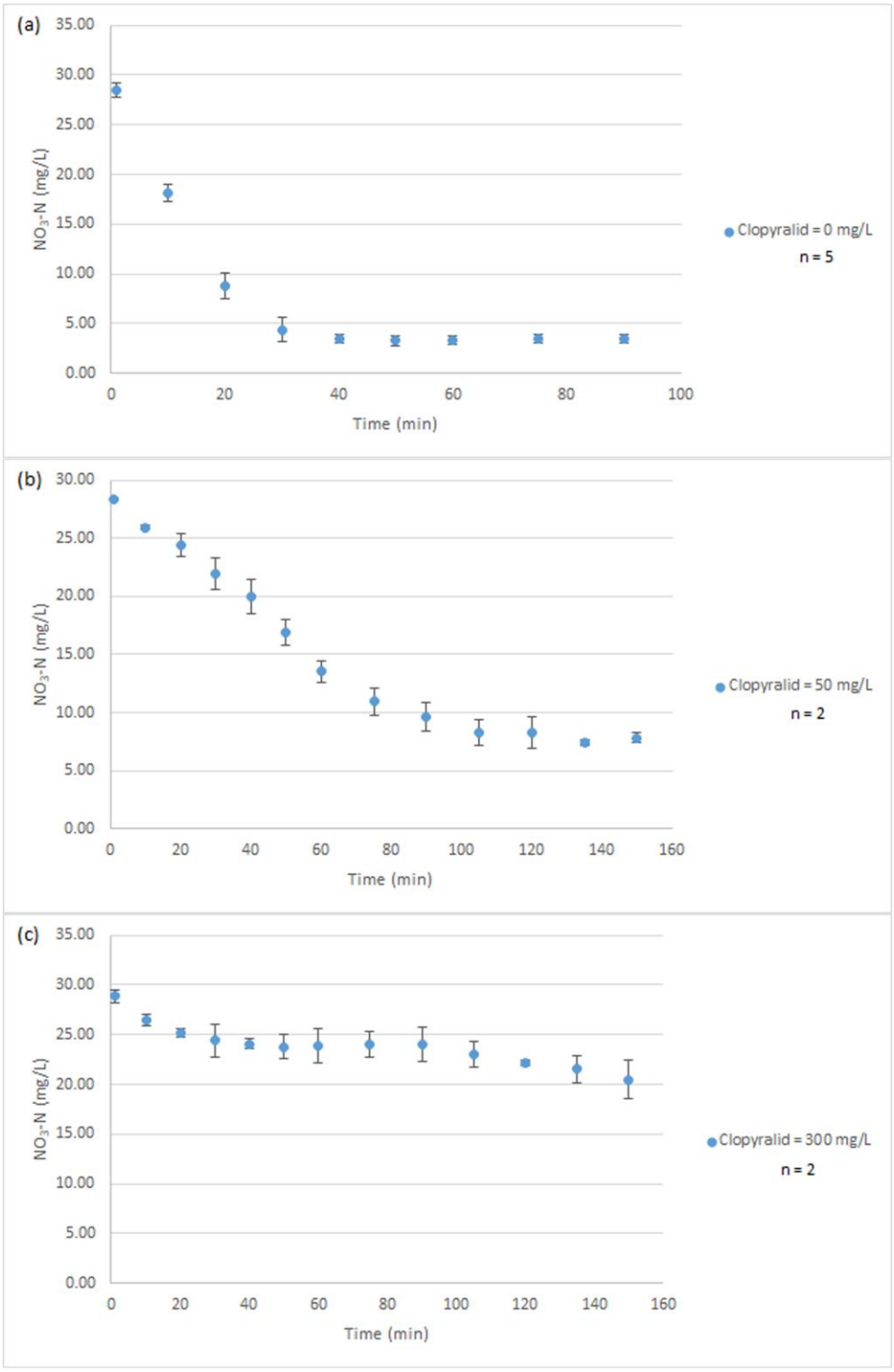

Figure 4.13: Results of batch tests with freely suspended cells under different clopyralid concentrations

4.4.2. Stage IV-1: Batch tests using encapsulated cells

Batch tests were then done using encapsulated cells under two different clopyralid concentrations (50 and 300 mg/L) to investigate the denitrification rates. The results of these tests are plotted in Figure 4.14 (b) & (c). As can be seen, nitrate removals were approximately 76 % and 41 %, respectively under 50 and 300 mg/L clopyralid, indicating the encapsulated cells were also able to remove the nitrates under these clopyralid concentrations. Comparing with the removals from freely-suspended-cell cases (i.e. Figure 4.13 (b) & (c)), cell encapsulation provided marginal protection against clopyralid. Additionally, in both cases, the NO_3-N concentration dropped instantly to approximately 25 mg/L after the addition of the nitrate feed which had been targeted to provide an initial concentration of about 28 mg/L (i.e. the same starting conditions as the free cell cases); however, the initial drops were not as much as that in the no-clopyralid case (i.e. Figure 4.14 (a)). Moreover, a 20-minute lag phase can be seen at the beginning of the 50 mg/L clopyralid cases; thus, the denitrification rate was only calculated for the declining portion of the data (generally from 20 to 90 minutes). The error bars in Figure 4.14 indicate the standard deviation of the replicates for each clopyralid concentration. Along with the measured VSS of the sludge, these results were used to determine the biomass-specific denitrification rates.

The error bars from 30 to 75 minutes in Figure 4.14 (c) indicate relatively large standard deviations making what happened during this period difficult to determine. Even though the mean values illustrated a slight decrease from 24 to 16 mg N/L from 30 to 75 minutes, the error bars do not allow the calculation of a denitrification rate.

To ensure consistency with previous discussions, zero-order model was also employed to describe the decrease of NO_3-N concentrations observed in Figure 4.14 (b). The zero-order reaction rate constant was 0.3 mg N/min for the 50 mg/L clopyralid data; while the biomass-specific denitrification rate was calculated to be 0.053 mg N/(g VSS·min). This denitrification rate was about the twice the rate found in the free-cell case (0.027 mg N/(g VSS·min)) (Figure 4.13 (b)). Consequently, the denitrification rate of the 50 mg/L clopyralid case was enhanced by cell encapsulation in the presence of clopyralid being substantially greater than the rate obtained with freely suspended cells.

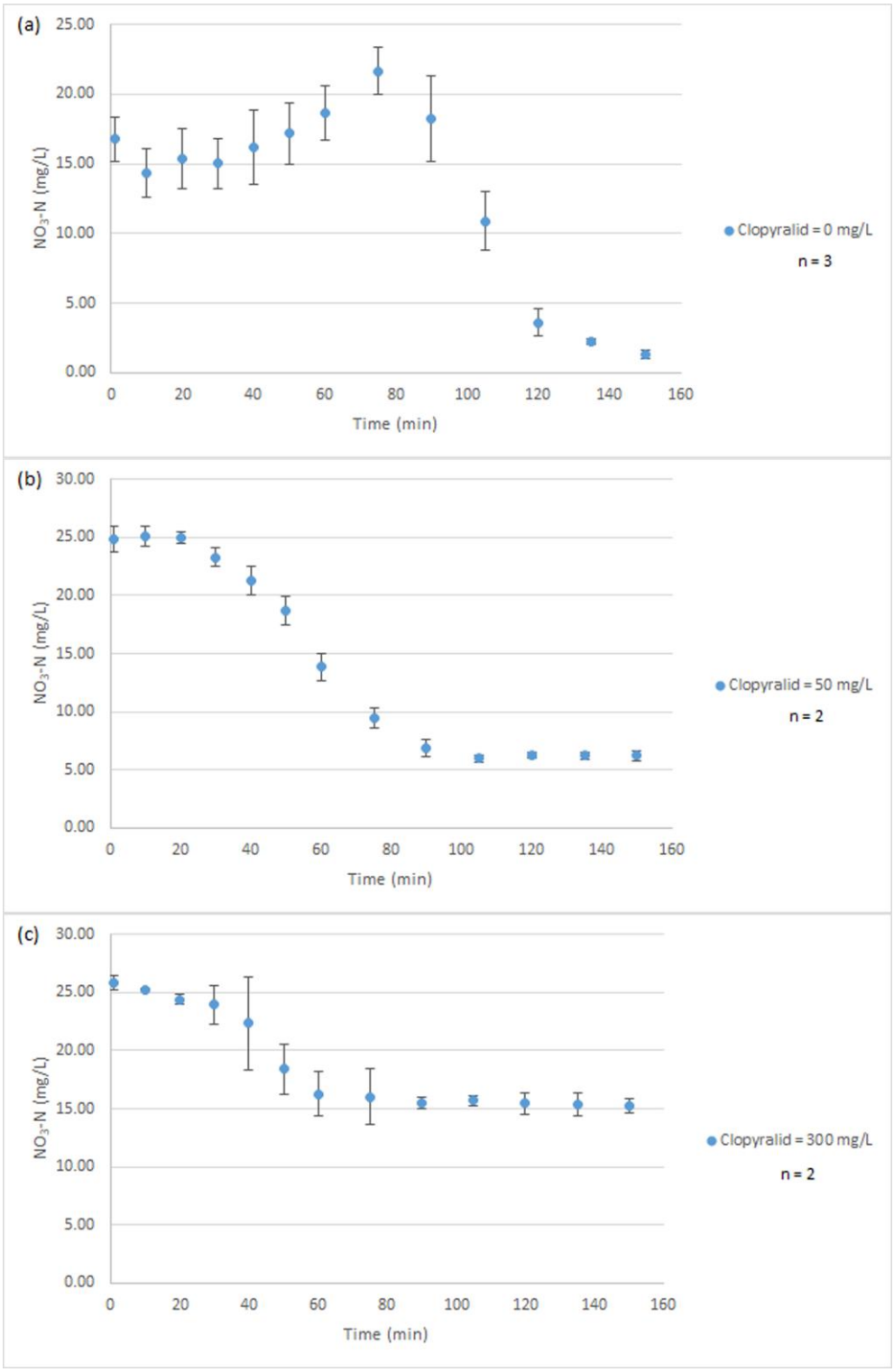

Figure 4.14: Results of batch tests with encapsulated cells under different clopyralid concentrations

5. Conclusions and recommendations

5.1. Conclusions

(1). In Phase I (the preliminary tests), the anoxic SBR failed to operate as a sludge generator to produce a healthy denitrifying biomass since the ORP in the SBR was regularly in the -300 mV range and the spikes of nitrate-nitrogen were observed in both sets of denitrification tests. Due to a reasonable biomass-specific denitrification rate of 0.114 mg N/(g VSS·min) which was comparable to other research, it was decided to collect sludge from the Pines WWTP which was then used for batch tests in Phase II, III, and IV.

(2). In Phase II (denitrification under different pH conditions), the neutral-pH denitrification rate was 0.113 mg N/(g VSS·min) which appeared to be close to the nitrate-removal rate of 0.12 mg N/(g VSS·min), as reported by Fernandez-Nava, Maranon, Soons & Castrillon (2008). The denitrification rates under pH 5.0 and pH 9.3 were found to be close to each other and both were approximately half the rate under neutral pH condition. The abiotic tests suggest there is some kind of adsorption or chemical reaction between the nitrates and the sodium-alginate beads because 48.8% - 92.5% of the initial nitrate was observed to be instantly "removed" upon contacts. According to the results of the batch tests using encapsulated cells, cell-encapsulation technology appeared to negatively affect the denitrification rate (under all pH conditions). Therefore, the biological denitrification process by free cells was negatively impacted under both high and low pH conditions and the cell-encapsulation technology did not provide protection against these suboptimal conditions.

(3). In Phase III (denitrification in the presence of nZVI), the results of preliminary and abiotic tests indicate there was basically no adsorption or chemical reaction between the nitrates, the nanoparticles and the sodium alginate. According to the batch tests using freely suspended cells, the biomass-specific denitrification rates were so close together (approximately 0.023 mg N/(g VSS·min)) in both 0.5 and 3 mg/L nZVI cases indicating the denitrification process was severely affected by the addition of nanoparticles. The results of the encapsulated-cell cases suggest that the denitrification rate of the 0.5 g/L nZVI case was further negatively affected by cell encapsulation in the presence of nanoparticles. Meanwhile, the effect on the denitrification rate of the 3 g/L nZVI case was difficult to evaluate due to the large standard deviations associated with the results. Accordingly, the biological denitrification process of free cells was negatively impacted under both nZVI concentrations; however, cell-encapsulation technology further impacted the denitrification rate in the 0.5 mg/L nZVI case.

(4). In Phase IV (denitrification in the presence of clopyralid), the results of the batch tests indicate that the denitrification performance of freely suspended cells was negatively affected at both high and low clopyralid concentrations. With the denitrification rate more severely impacted at the high clopyralid concentration than at low concentration. In contrast, the denitrification rate of the 50 mg/L clopyralid case was found to be marginally enhanced by cell encapsulation technology.

5.2. Recommendations

(1). The potential adsorption or chemical reaction between the nitrates and the sodium alginate should be further investigated.

(2). As the high pH buffer failed to modify and control the pH at around 9.3 in the batch tests using encapsulated cells, further investigation should be carried out to find out the reason for this failure and other ways to maintain the pH at about 9.3 in the presence of encapsulated cells.

(3). Other parameters (COD, nitrite, pH, Fe^{2+}, clopyralid concentration) can be tracked during batch tests to develop a comprehensive understanding of the effects on denitrification caused by pH, nZVI and clopyralid.

(4). Other kinetic models can be trailed to see if they have a better fit to the experimental data.

6. References

Agrawal, A., Tratnyek, P. G. (1996). Reduction of nitro aromatic compounds by zero-valent iron metal. *Environ. Sci. Technol. 30*, 153–160.

Ali, M., & Okabe, S. (2015, Dec). Anammox-based technologies for nitrogen removal: Advances in process start-up and remaining issues. *Chemosphere, 141*, 144-153. https://doi.org/10.1016/j.chemosphere.2015.06.094

Alowitz, M. J., Scherer, M. M. (2002). Kinetics of nitrate, nitrite, and Cr(VI) reduction by iron metal. *Environ. Sci. Technol. 36*, 299–306.

Aslan, Ş., & Türkman, A. (2005). Combined biological removal of nitrate and pesticides using wheat straw as substrates. *Process Biochemistry, 40*(2), 935-943. doi: 10.1016/j.procbio.2004.02.020

Artan, N., Orhon, D. (2005). International Water Association, & IWA Specialist Group on Nutrient Removal and Recovery. Mechanism and design of sequencing batch reactors for nutrient removal. London: IWA Pub.

Australian and New Zealand Guidelines for Fresh and Marine Water Quality. (2000). Retrieved from https://www.waterquality.gov.au/sites/default/files/documents/anzecc-armcanz-2000-guidelines-vol1.pdf

Barth, E. F. (1972). Design of treatment facilities for the control of nitrogenous materials. *Water Research Pergamon Press, vol. 6*, 481-483.

Burghate, S. P., & Ingole, D. W., (2014). Biological Denitrification- a Review. *International Journal of Research in Environmental Science and Technology, 3*, 78-85.

Cao, X., Qian, D., & Meng, X. (2013). Effects of pH on nitrite accumulation during wastewater denitrification. *Environmental technology, 34*(1), 45-51. doi:10.1080/09593330.2012.679700

Chen, C. Y., Kao, C. M., Chen, S. C., Chien, H. Y., & Lin, C. E. (2007). Application of immobilized cells to the treatment of cyanide wastewater. *Water Sci Technol, 56*(7), 99-107. doi: 10.2166/wst.2007.699

Chevalier, P., & de la Noüe, J. (1985). Wastewater nutrient removal with microalgae immobilized in carrageenan. *Enzyme and Microbial Technology, 7*(12), 621-624. https://doi.org/https://doi.org/10.1016/0141-0229(85)90032-8

Chew, C. F., Zhang, T. C. (1998). In situ remediation of nitrate-contaminated ground water by electrokinetics/iron wall processes. *Water Sci. Technol. 38*, 135–142.

Choe, S., Chang, Y. Y., Hwang, K. Y., Khim, J. (2000). Kinetics of reductive denitrification by nanoscale zero-valent iron. *Chemosphere, 41*(8), 1307–1311.

Dosta, J., Fernandez, I., Vazquez-Padin, J.R., Mosquera-Corral, A., Campos, J.L., Mata-Alvarez, J. & Mendez, R. (2008). Short- and long-term effects of temperature on the Anammox process. *J. Hazard. Mater, 154*, 688–693.

de la Noue, J., & de Pauw, N. (1988). The potential of microalgal biotechnology: A review of production and uses of microalgae. *Biotechnology Advances, 6*(4), 725-770. doi: https://doi.org/10.1016/0734-9750(88)91921-0

de-Bashan, L. E., & Bashan, Y. (2010). Immobilized microalgae for removing pollutants: review of practical aspects. *Bioresour Technol, 101*(6), 1611-1627. doi: 10.1016/j.biortech.2009.09.043

Dong, Q., Parker, W., & Dagnew, M. (2016). Influence of SRT and HRT on Bioprocess Performance in Anaerobic Membrane Bioreactors Treating Municipal Wastewater. *Water Environ Res, 88*(2), 158-167. doi: 10.2175/106143016X14504669767175

Eaton, A. D., Clesceri, L. S., Greenberg, A. E., & Franson, M. A. H. (2005). Standard methods for the examination of water and wastewater. 21th ed. 2005. Washington, DC: American Public Health Association.

Environment Canterbury. (2018). Annual Groundwater Quality Survey. Retrieve from https://api.ecan.govt.nz/TrimPublicAPI/documents/download/3588758

Fernandez-Nava, Y., Maranon, E., Soons, J., & Castrillon, L. (2008). Denitrification of wastewater containing high nitrate and calcium concentrations. *Bioresour Technol, 99*(17), 7976-7981. doi:10.1016/j.biortech.2008.03.048

Flis, J. (1991). Stress corrosion cracking of structural steels in nitrate solutions. In:Flis, J. (Ed.), Corrosion of Metals and Hydrogen-Related Phenomena. *Materials Science Monograph, 59*. Elsevier, Amsterdam, NL, pp. 57–94.

Glass, C., & Silverstein, J. (1998). Denitrification kinetics of high nitrate concentration water: pH effect on inhibition and nitrite accumulation. *Water Research, 32*(3), 831-839. doi:https://doi.org/10.1016/S0043-1354(97)00260-1

Gonzalez-Olmos, R. (2015). Leading edge technologies in wastewater treatment. *AIMS Environmental Science, 2*(2), 237-240. doi: 10.3934/environsci.2015.2.237

Han, Y., Zhang, W., Lu, W., Zhou, Z., Zhuang, Z., & Li, M. (2014). Co-immobilization of Pseudomonas stutzeri YHA-13 and Alcaligenes sp. ZGED-12 with polyvinyl alcohol-alginate for removal of nitrogen and phosphorus from synthetic wastewater. *Environ Technol, 35*(21-24), 2813-2820. doi: 10.1080/09593330.2014.923516

Hill, C. B., & Khan, E. (2008). A Comparative Study of Immobilized Nitrifying and Co-Immobilized Nitrifying and Denitrifying Bacteria for Ammonia Removal from Sludge Digester Supernatant. *Water, Air, and Soil Pollution, 195*(1-4), 23-33. doi: 10.1007/s11270-008-9724-x

Hu, H. Y., Iwasaki, M., Fujie, K., Goto, N., Kasakura, T., He, Y. M., Tsubone, T. (1999). Chemical reduction of nitrate and nitrite in aquatic solution by zero-valent metals. In: *Proceedings of Asian Waterqual '99-7th IAWQ Asia-Pacific Regional Conference*, 18–20 October. Taipei, Taiwan, pp. 553–558.

Huang, Y. H., Zhang, T. C. (2002). Kinetics of nitrate reduction by iron at near neutral pH. J. *Environ. Eng. 128*, 604–611.

Huang, Y. H., Zhang, T. C. (2004). Effects of low pH on nitrate reduction by iron powder. *Water Res. 38*, 2631–2642.

Huang, Z., Ong, S. L., & Ng, H. Y. (2011). Submerged anaerobic membrane bioreactor for low-strength wastewater treatment: effect of HRT and SRT on treatment performance and membrane fouling. *Water Res, 45*(2), 705-713. doi: 10.1016/j.watres.2010.08.035

Hura, A. K. (2019). *Biological treatment of industrial strength clopyralid in wastewaters: biodegradation & toxicity* (Doctoral thesis, University of Canterbury, Christchurch, New Zealand). Retrieved from https://ir.canterbury.ac.nz/handle/10092/16835

Jenkins, D., & Wanner, J. (2014). *Activated Sludge - 100 Years and Counting: 100 Years and Counting*. London, United Kingdom: IWA Publishing.

Kartal, B., de Almeida, N.M., Maalcke, W.J., Op den Camp, H.J.M., Jetten, M.S.M., Keltjens, J.T. 2013. How to make a living from anaerobic ammonium oxidation. *FEMS Microbiol.* Rev. 37, 428–461.

Khan, H., & Bae, W. (2014). Rapid start-up and efficient long-term nitritation of low strength ammonium wastewater with a sequencing batch reactor containing immobilized cells. *Water Sci Technol, 70*(3), 517-523. doi: 10.2166/wst.2014.251

Kielemoes, J., de Boever, P., Verstraete, W. (2000). Influence of denitrification on the corrosion of iron and stainless-steel powder. *Environ. Sci. Technol. 34*, 663–671.

Lau, P. S., Tam, N. F. Y., & Wong, Y. S. (1997). Wastewater Nutrients (N and P) Removal by Carrageenan and Alginate Immobilized Chlorella Vulgaris. *Environmental Technology, 18*(9), 945-951. doi: 10.1080/09593331808616614

Lee, P. G., Lea, R. N., Dohmann, E., Prebilsky, W., Turk, P. E., Ying, H., & Whitson, J. L. (2000). Denitrification in aquaculture systems: an example of a fuzzy logic control problem. *Aquacultural Engineering, 23*(1), 37-59. doi:https://doi.org/10.1016/S0144-8609(00)00046-7

Liu, K., Li, J., Qiao, H., Lin, A., & Wang, G. (2012). Immobilization of Chlorella sorokiniana GXNN 01 in alginate for removal of N and P from synthetic wastewater. *Bioresour Technol, 114*, 26-32. doi: 10.1016/j.biortech.2012.02.003

Llop, A., Pocurull, E., & Borrull, F. (2008). Evaluation of the Removal of Pollutants from Petrochemical Wastewater Using a Membrane Bioreactor Treatment Plant. *Water, Air, and Soil Pollution, 197*(1-4), 349-359. doi: 10.1007/s11270-008-9816-7

Lu, C., Mei Lee, C., Ming Lu, W., & Chen, P. (1994). A model of nitrogen removal in waste-waters using alginate-entrapped cyabobacteria anabaena Ch3. *Environment International, 20*(4), 529-540. doi:10.1016/0160-4120(94)90201-1

Lu, Y., Ma, L., Liang, Y., Shan, B., & Chang, J. (2018). Enhancing Nitrogen Removal Performance in a Bioreactor Using Immobilized Anaerobic Ammonium Oxidation Sludge by Polyvinyl Alcohol-Sodium Alginate (PVA-SA). *Polish Journal of Environmental Studies, 27*(2), 773-778. doi: 10.15244/pjoes/75805

Mackenzie, L., Davis, D., A., C. (1998). Introduction to Environment al Engineering (Third Edition).

Mallick, N. (2002). Biotechnological potential of immobilized algae for wastewater N, P and metal removal: A review. *BioMetals* (15), 377–390.

McIlvaine, T. C. (1921). A buffer solution for colorimetric comparison. *J. Biol. Chem. 49* (1): 183–186.

Ministry for the Environment (2007). Environment New Zealand 2007. Retrieved from https://www.mfe.govt.nz/sites/default/files/environment-nz07-dec07.pdf

Mulder, A., Van De Graaf, A. A., Robertson, L. A., & Kuenen, J. G. (1995). Anaerobic ammonium oxidation discovered in a denitrifying fluidized bed reactor. *FEMS Microbiology Ecology, 16*(3), 177-184.

Nagaoka, H. (1999). Nitrogen removal by submerged membrane separation activated sludge process. *Water Science and Technology, 39*, 107-114.

Ni, S., Sung, S., Yue, Q. & Gao, B. (2012). Substrate removal evaluation of granular anammox process in a pilot-scale upflow anaerobic sludge blanket reactor. *Ecol. Eng., 38*, 30–36.

Op den Camp, H. J. M., Jetten, M. S. M., & Strous, M. (2007). Chapter 16 - Anammox. In H. Bothe, S. J. Ferguson, & W. E. Newton (Eds.), *Biology of the Nitrogen Cycle*, 245-262. Amsterdam: Elsevier.

Pan, Y., Ye, L., Ni, B. J., & Yuan, Z. (2012). Effect of pH on N_2O reduction and accumulation during denitrification by methanol utilizing denitrifiers. *Water Res, 46*(15), 4832-4840. doi:10.1016/j.watres.2012.06.003

Parliamentary Commissioner for the Environment (2013). Water quality in New Zealand: Land use and nutrient pollution. Retrieved from https://www.pce.parliament.nz/media/1275/pce-water-quality-land-use-web-amended.pdf

Perez-Garcia, O., Ng, F., Singhal, N. & Bickers, P. (2018). A utilities' guide to starting up ANAMMOX. *WaterNZ*.

Pramanik, S., & Khan, E. (2008). Effects of cell entrapment on growth rate and metabolic activity of mixed cultures in biological wastewater treatment. *Enzyme and Microbial Technology, 43*(3), 245-251. doi: 10.1016/j.enzmictec.2008.04.004

Pramanik, S., McEvoy, J., Siripattanakul, S., & Khan, E. (2011). Effects of cell entrapment on nucleic acid content and microbial diversity of mixed cultures in biological wastewater treatment. *Bioresour Technol, 102*(3), 3176-3183. doi: 10.1016/j.biortech.2010.10.133

Qiu, Y., Shi, H.-c., & He, M. (2010). Nitrogen and Phosphorous Removal in Municipal Wastewater Treatment Plants in China: A Review. *International Journal of Chemical Engineering, 2010*, 1-10. doi: 10.1155/2010/914159

Richards, F. A. (1965). Anoxic basins and fjordsin. *Chemical Oceanography*, J.P. Ripley and G. Skirrow, Eds., pp 611-645, Academic Press, London, UK.

Ruiz-Marin, A., Mendoza-Espinosa, L. G., & Stephenson, T. (2010). Growth and nutrient removal in free and immobilized green algae in batch and semi-continuous cultures treating real wastewater. *Bioresour Technol, 101*(1), 58-64. doi: 10.1016/j.biortech.2009.02.076

Sergio A. Covarrubias, L. E. d.-B., Manuel Moreno & Yoav Bashan. (2012). Alginate beads provide a beneficial physical barrier against native microorganisms in wastewater treated with immobilized bacteria and microalgae. *ENVIRONMENTAL BIOTECHNOLOGY, 93*, 2669–2680. doi: 10.1007/s00253-011-3585-8)

Shchegolkova, N. M., Krasnov, G. S., Belova, A. A., Dmitriev, A. A., Kharitonov, S. L., Klimina, K. M., & Kudryavtseva, A. V. (2016). Microbial Community Structure of Activated Sludge in Treatment Plants with Different Wastewater Compositions. *Frontiers in Microbiology, 7*. https://doi.org/10.3389/fmicb.2016.00090

Siantar, D., Schreier, C. G., Chou, C. S., Reinhard, M. (1996). Treatment of 1,2-dibromo-3-chloroproprane and nitrate contaminated water with zero-valent iron or hydrogen/ palladium catalysts. *Water Res. 30*(10), 2315–2322.

Skiba, U. (2008). Denitrification. In S. E. Jørgensen & B. D. Fath (Eds.), *Encyclopedia of Ecology* (pp. 866-871). Oxford: Academic Press.

Sobieszuk, P., & Szewczyk, K. (2006). Estimation of (C/N) Ratio for Microbial Denitrification. *Environmental technology, 27*, 103-108. doi:10.1080/09593332708618624

Till, B. A., Weathers, L. J., Alvarez, P. J. J. (1998). Fe(0)-supported autotrophic denitrification. *Environ. Sci. Technol. 32*, 634–639.

Vackova, L., Stloukal, R., & Wanner, J. (2012). The possibility of using encapsulated nitrifiers for treatment of reject water coming from anaerobic digestion. *Water Sci Technol, 65*(8), 1428-1434. doi: 10.2166/wst.2012.028

Vílchez, C., & Vega, J. M. (1994). Nitrate uptake by Chlamydomonas reinhardii cells immobilized in calcium alginate. *Applied Microbiology Biotechnology Advances, 41*, 137-141.

Wilderer, P. A., Irvine, R. L., & Goronszy, M. C. (2001). Sequencing batch reactor technology. London: IWA Pub.

Yang, G. C., & Lee, H. L. (2005). Chemical reduction of nitrate by nanosized iron: kinetics and pathways. *Water Res, 39*(5), 884-894. doi:10.1016/j.watres.2004.11.030

Young, G. K., Bungay, H. R., Brown, L. M., Parsons, W. A. (1964). Chemical reduction of nitrate in water. *J. Water Pollut. Control Federation 36*, 395–398.

Yoo, Y. J., Hwang, D. H., & Sohn, D. S. (1999). Development of a subchannel analysis code MATRA applicable to PWRs and ALWRs. *J. Korean Nucl. Soc., 31*(3), 314-327.

Zhao, J., Yang, Q., Li, X., Wang, D., An, H., Xie, T., Xu, Q., Deng, Y., Zeng, G. (2015). Effect of initial pH on short chain fatty acid production during the anaerobic fermentation of membrane bioreactor sludge enhanced by alkyl polyglcoside. *International Biodeterioration & Biodegradation, 104*, 283-289. doi: 10.1016/j.ibiod.2015.06.012

Appendix. Raw Data

This appendix presents the raw data associate to the figures in the Result and Discussion chapter.

List of Sections

Phase I: Preliminary Tests

Table A.1: Profile of TSS in the SBR

Day	TSS (mg/L)	Day	TSS (mg/L)
1	1610	32	3340
2	1610	33	3410
3	1590	34	3700
4	1520	35	3670
5	1710	36	3520
6	1550	37	3880
7	1870	38	3530
8	1750	39	2490
9	1430	40	4430
10	1350	41	4390
11	1860	42	3690
12	1930	43	4120
13	1740	44	4230
14	1850	45	3960
15	1890	46	3890
16	2080	47	4180
17	2180	48	4490
18	2170	49	4740
19	2350	50	4120
20	2120	51	4300
21	2330	52	4680
22	2140	53	4240
23	2390	54	5580
24	2740	55	4650
25	2510	56	4100
26	2720	57	4360
27	2010	58	4060
28	2300	59	5620
29	2510	60	4480
30	2700	61	4050
31	2880		

Table A.2: NO_3-N concentration changes with time in the SBR

Time (min)	NO_3-N (mg/L)					
0	28.1	28.1	28.3	28.1	28.2	28.4
10	18.6	18.9	19.1	17.6	18.1	16.2
20	28.9	29.1	28.3	27.9	28.1	28.6
30	10.8	12.1	9.9	8.6	10.6	11.3
40	3.3	5.6	2.5	2.9	3.3	3.1
50	0.9	1.2	0.9	0.8	0.9	0.9
60	0.7	0.8	0.9	0.9	0.7	0.8
75	0.8	0.9	0.9	0.8	0.9	0.9
90	0.8	0.8	0.9	0.6	0.8	0.9

Table A.3: Results of the 500-mL denitrification batch tests using sludge from SBR

Time (min)	NO_3-N (mg/L)		
0	2.0	2.6	2.3
10	23.7	25.9	25.1
20	34.3	28.1	31.1
30	20.9	23.2	19.8
40	10.1	9.4	9.9
50	3.4	2.7	3.0
60	2.7	2.7	2.7
75	2.8	2.9	2.5
90	2.9	3.1	2.3

Table A.4: Profile of ORP in the SBR

Time (min)	ORP (mV)	Time (min)	ORP (mV)	Time (min)	ORP (mV)
0.7	-170.532	30.7	-381.0391	60.7	-425.5807
1.7	-186.449	31.7	-384.5214	61.7	-425.5807
2.7	-200.8587	32.7	-387.7957	62.7	-425.5807
3.7	-209.7852	33.7	-390.9272	63.7	-425.5807
4.7	-217.3214	34.7	-393.9157	64.7	-425.5807
5.7	-224.2470	35.7	-396.9301	65.7	-425.5807
6.7	-232.0430	36.7	-399.7237	66.7	-425.5807
7.7	-239.2284	37.7	-402.5693	67.7	-425.5807
8.7	-246.3878	38.7	-405.3109	68.7	-425.5807
9.7	-254.5737	39.7	-408.0915	69.7	-425.5807
10.7	-261.9930	40.7	-410.8981	70.7	-425.5807
11.7	-268.8016	41.7	-413.6008	71.7	-425.5807
12.7	-275.8570	42.7	-416.3424	72.7	-425.5807
13.7	-283.0164	43.7	-419.1490	73.7	-425.5807
14.7	-288.3827	44.7	-422.0465	74.7	-425.5807
15.7	-294.3727	45.7	-424.9571	75.7	-425.5807
16.7	-300.8305	46.7	-425.5807	76.7	-425.5807
17.7	-306.5606	47.7	-425.5807	77.7	-425.5807
18.7	-312.7195	48.7	-425.5807	78.7	-425.5807
19.7	-318.7095	49.7	-425.5807	79.7	-425.5807
20.7	-324.9333	50.7	-425.5807	80.7	-425.5807
21.7	-331.5860	51.7	-425.5807	81.7	-425.5807
22.7	-338.6025	52.7	-425.5807	82.7	-425.5807
23.7	-345.5020	53.7	-425.5807	83.7	-425.5807
24.7	-352.1417	54.7	-425.5807	84.7	-425.5807
25.7	-358.2096	55.7	-425.5807	85.7	-425.5807
26.7	-363.6019	56.7	-425.5807	86.7	-425.5807
27.7	-368.7733	57.7	-425.5807	87.7	-425.5807
28.7	-373.2301	58.7	-425.5807	88.7	-425.5807
29.7	-377.2061	59.7	-425.5807	89.7	-425.5807

Table A.5: Results of the denitrification batch tests using sludge from Pines WWTP

Time (min)	NO_3-N (mg/L)				
0	29.1	27.7	28.3	27.9	29.4
10	18.9	17.2	17.9	17.6	19.1
20	11	8.5	7.7	8.3	8.5
30	6.6	4.4	3.3	3.9	3.9
40	3.6	3.9	3.3	3.9	2.9
50	2.9	3.6	3.0	4.0	3.0
60	3.0	3.6	3.1	3.9	3.1
75	3.1	3.7	3.2	4.1	3.1
90	3.2	3.8	3.3	4.2	3.2

Phase II: Denitrification Rates Under Different pH Conditions

Stage II-1: Batch tests using freely suspended cells

Table A.6: Results of batch tests with freely suspended cells under neutral pH condition

Time (min)	NO_3-N (mg/L)														
0	29.1	27.7	28.3	27.9	29.4	28.8	27.7	28	29.3	27.7	29	27.8	27.7	28.5	25.9
10	18.9	17.2	17.9	17.6	19.1	18.1	17.1	17.5	19.1	18.2	20.3	18.9	19	20.3	16.7
20	11	8.5	7.7	8.3	8.5	9.7	7.9	8.5	10.7	6.7	12.3	10.5	12.1	11.1	4.5
30	6.6	4.4	3.3	3.9	3.9	4.5	3.0	3.2	7.7	3.8	6.1	4.7	6.4	4.4	3.1
40	3.6	3.9	3.3	3.9	2.9	3.9	2.9	3.1	3.9	4.0	3.3	3.3	3.4	3.8	3.2
50	2.9	3.6	3.0	4.0	3.0	2.9	3.0	3.0	4.0	3.0	3.3	3.3	3.5	3.9	3.2
60	3.0	3.6	3.1	3.9	3.1	3.0	3.0	3.1	4.0	3.1	3.2	3.1	3.6	4.0	3.3
75	3.1	3.7	3.2	4.1	3.1	3.0	3.1	3.1	4.2	3.2	3.3	3.3	3.7	4.0	3.4
90	3.2	3.8	3.3	4.2	3.2	3.1	3.2	3.0	4.4	3.2	3.4	3.3	3.7	4.1	3.5

Table A.7: Results of batch tests with freely suspended cells under low pH condition

Time (min)	NO_3-N (mg/L)				
0	27.3	27.5	38.6	36.9	33.4
10	23.4	24.1	18.3	28.9	26.7
20	21.1	21.0	13.0	21.7	19.1
30	19.7	19.1	16.1	14.4	13.4
40	16.5	15.9	7.3	9.1	10.0
50	15.9	11.4	5.2	6.7	7.3
60	9.4	8.7	4.2	5.3	6.1
75	6.6	5.1	3.2	4.6	5.0
90	5.9	4.1	3.2	3.9	3.9

Table A.8: Results of batch tests with freely suspended cells under high pH condition

Time (min)	NO_3-N (mg/L)			
0	29.4	27.6	30.9	29.5
10	27.0	25.5	28.1	27.7
20	23.4	21.7	25.1	24.9
30	19.1	18.7	21.3	21.1
40	14.3	13.5	17.7	16.5
50	11.1	10.1	15.1	11.3
60	8.1	7.3	9.9	7.4
75	7.2	5.3	7.5	6.6
90	5.1	4.3	5.1	5.4
105	4.5	4.1	4.1	4.5
120	4.3	4.5	4.0	4.1

Stage II-2: Abiotic tests

Table A.9: Results of batch tests with blank sodium-alginate beads under neutral pH condition

Time (min)	NO_3-N (mg/L)		
0	19.8	20.4	19.5
10	18.9	20.1	17.9
20	17.5	19.1	18.1
30	18.1	19.8	18.8
40	18.2	18.9	18.1
50	18.7	18.7	17.7
60	17.6	19.5	17.0
75	17.6	18.9	17.5
90	18.5	18.5	17.6
105	18.5	19.0	18.2
120	17.4	19.1	17.9

Table A.10: Results of batch tests with blank sodium-alginate beads under low pH condition

Time (min)	NO_3-N (mg/L)		
0	1.5	1.6	1.1
10	1.6	1.0	1.3
20	1.3	1.2	1.4
30	1.0	1.3	1.3
40	1.1	1.2	1.2
50	1.2	1.3	1.3
60	1.1	1.4	1.4
75	1.3	1.3	1.3
90	1.3	1.4	1.3
105	1.2	1.5	1.2
120	1.4	1.1	1.3
135	1.7	1.3	1.4
150	1.3	1.2	1.1

Table A.11: Results of batch tests with blank sodium-alginate beads under high pH condition

Time (min)	NO_3-N (mg/L)		
0	17.0	15.7	16.4
10	16.7	13.2	15.0
20	15.5	13.5	14.3
30	14.6	13.6	13.5
40	14.5	13.2	13.3
50	14.8	14.3	14.2
60	13.9	14.2	13.4
75	14.9	13.3	13.7
90	14.9	13.2	14.3
105	14.8	13.2	14.2
120	15.0	13.9	13.7
135	14.2	13.3	13.8
150	14.2	13.0	13.7

Stage II-3: Batch tests using encapsulated cells

Table A.12: Results of batch tests with encapsulated cells under neutral pH condition

Time (min)	NO_3-N (mg/L)		
0	15.1	16.9	18.3
10	13.4	13.3	16.4
20	13.6	14.8	17.7
30	13.9	14.1	17.1
40	15.5	13.9	19.1
50	15.3	16.7	19.6
60	18.3	20.7	16.9
75	22.1	23.1	19.8
90	14.7	19.9	20.1
105	8.5	12.1	12.1
120	3.3	4.7	2.8
135	2.4	2.1	2.1
150	1.5	1.1	1.2

Table A.13: Results of batch tests with encapsulated cells under low pH condition

Time (min)	NO_3-N (mg/L)		
0	1.9	3.0	1.6
10	2.1	3.2	2.0
20	2.8	3.9	2.7
30	3.1	5.4	2.9
40	4.1	5.2	3.6
50	5.1	5.4	4.4
60	5.4	5.8	4.9
75	6.7	6.6	5.7
90	8.3	7.3	6.5
105	8.5	7.9	7.0
120	9.4	8.6	8.1
135	9.3	9.2	8.5
150	9.4	9.6	9.4

Table A.14: Results of batch tests with encapsulated cells under high pH condition

Time (min)	NO_3-N (mg/L)		
0	5.1	5.7	6.7
10	4.9	5.2	5.9
20	5.9	5.7	5.8
30	6.3	6.4	5.7
40	7.1	6.3	6.2
50	8.2	6.9	6.8
60	8.8	7.8	7.7
75	9.0	7.9	8.5
90	9.8	8.9	8.9
105	10.1	9.1	9.0
120	7.0	9.3	7.2
135	2.1	5.1	2.6
150	1.2	1.6	1.5

Phase III: Denitrification Rates under Different nZVI Concentrations

Stage III-1: Baseline tests

Table A.15: Results of batch tests under 0.5 mg/L nZVI without biomass

Time (min)	NO_3-N (mg/L)	
0	28.2	28.4
10	27.5	28.1
20	27.6	28.1
30	28.5	27.9
40	28.7	28.0
50	29.5	27.5
60	28.5	27.7
75	28.5	28.1
90	29.5	28.2
105	25.7	28.4
120	29.8	28.7
135	29.6	28.5
150	29.8	28.3

Table A.16: Results of batch tests under 3 mg/L nZVI without biomass

Time (min)	NO_3-N (mg/L)	
0	29.1	28.7
10	28.4	28.5
20	29.8	28.3
30	29.9	28.4
40	27.5	28.1
50	28.3	27.9
60	26.8	28.0
75	29.4	28.1
90	27.7	28.2
105	29.9	28.0
120	29.8	27.7
135	29.5	27.5
150	29.6	27.8

Stage III-2: Batch tests using freely suspended cells

Table A.17: Results of batch tests with freely suspended cells under 0.5 mg/L nZVI

Time (min)	NO_3-N (mg/L)		
0	21.7	25	12.9
10	22.9	21.8	15.2
20	20.3	23.6	13
30	18.8	19	17
40	20.6	18	16.9
50	15.8	14.5	17
60	12.4	12.7	15.5
75	10.8	9.9	13
90	10.2	6.7	12.1
105	10.7	2.8	11.1
120	8.8	1.7	9.5
135	10.9	1.3	8.3
150	10.8	1.4	6.7

Table A.18: Results of batch tests with freely suspended cells under 3 mg/L nZVI

Time (min)	NO_3-N (mg/L)		
0	22.5	26.3	13.7
10	22.3	26.8	15.1
20	20.1	24.4	15.5
30	24.9	22.1	19.4
40	21.2	19.6	18.3
50	18.8	16.8	18.2
60	18.4	14.3	19.4
75	18	11	15.6
90	17.6	7.5	14.2
105	18.2	1.6	12.9
120	19	1.5	10.3
135	14.9	1.4	9.1
150	18.5	1.4	7.3

Stage III-3: Abiotic tests

Table A.19: Results of batch tests with blank sodium-alginate beads under 0.5 mg/L nZVI

Time (min)	NO_3-N (mg/L)	
0	25.7	26.4
10	25.8	26.3
20	25.4	26.1
30	26.1	26.0
40	26.0	26.2
50	25.9	26.5
60	26.1	26.4
75	26.5	26.7
90	26.4	26.6
105	26.7	26.9
120	26.9	27.1
135	26.8	27.1
150	26.6	27.0

Table A.20: Results of batch tests with blank sodium-alginate beads under 3 mg/L nZVI

Time (min)	NO_3-N (mg/L)	
0	27.8	26.9
10	27.5	26.6
20	27.9	26.7
30	28.1	26.1
40	28.2	26.2
50	27.8	26.1
60	27.7	26.5
75	25.6	26.3
90	27.1	26.0
105	27.3	25.5
120	27.2	25.3
135	27.2	25.2
150	27.1	25.4

Stage III-4: Batch tests using encapsulated cells

Table A.21: Results of batch tests with encapsulated cells under 0.5 mg/L nZVI

Time (min)	NO_3-N (mg/L)	
0	22.8	26.4
10	20.6	23.8
20	23.6	21.6
30	20.0	20.5
40	18.7	22.5
50	19.8	24.6
60	21.1	20.9
75	18.4	19.9
90	21.0	18.4
105	18.0	18.9
120	19.0	21.2
135	17.2	17.0
150	17.1	16.6
165	17.2	15.7
180	15.0	16.5
195	15.5	16.3
210	14.9	15.5

Table A.22: Results of batch tests with encapsulated cells under 3 mg/L nZVI

Time (min)	NO_3-N (mg/L)	
0	24.6	27.3
10	27.2	28.1
20	27.9	28.4
30	23.1	30.2
40	28.4	28.5
50	23.4	29.4
60	25.5	30.2
75	22.8	31.9
90	22.5	30.2
105	23.3	29.6
120	20.9	27.3
135	20.6	26.1
150	18.4	24.9
165	18.9	24.5
180	16.9	25.5
195	17.1	26.1
210	17.3	25.8

Phase IV: Denitrification Rates under Different Clopyralid Concentrations

Stage IV-1: Batch tests using freely suspended cells

Table A.23: Results of batch tests with freely suspended cells under 50 mg/L clopyralid

Time (min)	NO_3-N (mg/L)	
0	28.5	28.3
10	26.1	25.8
20	25.1	23.7
30	22.9	21.0
40	21.0	18.9
50	17.7	16.1
60	14.2	12.9
75	11.8	10.1
90	10.5	8.8
105	9.1	7.5
120	9.2	7.3
135	7.3	7.6
150	7.5	8.1

Table A.24: Results of batch tests with freely suspended cells under 300 mg/L clopyralid

Time (min)	NO_3-N (mg/L)	
0	29.3	28.4
10	26.9	26.1
20	25.5	24.9
30	25.6	23.2
40	24.4	23.7
50	24.7	22.9
60	25.1	22.7
75	25.0	23.1
90	25.3	22.8
105	23.9	22.1
120	22.0	22.4
135	20.6	22.5
150	19.1	21.9

Stage IV-2: Batch tests using encapsulated cells

Table A.25: Results of batch tests with encapsulated cells under 50 mg/L clopyralid

Time (min)	NO_3-N (mg/L)	
0	24.1	25.6
10	24.5	25.7
20	25.3	24.6
30	23.9	22.7
40	22.1	20.4
50	19.6	17.8
60	14.7	13.0
75	10.1	8.9
90	7.4	6.3
105	5.7	6.2
120	6.1	6.4
135	6.0	6.4
150	5.9	6.5

Table A.26: Results of batch tests with freely encapsulated cells under 300 mg/L clopyralid

Time (min)	NO_3-N (mg/L)	
0	25.6	25.4
10	25.7	25.2
20	24.6	24.1
30	22.7	22.8
40	20.4	19.5
50	17.8	16.9
60	13.0	14.9
75	8.9	14.3
90	6.3	15.1
105	6.2	15.4
120	6.4	14.8
135	6.4	14.7
150	6.5	14.8